

1    **Research area:**  
2    abiotic stress - flooding/submergence  
3    phytoremediation  
4    transcriptional regulation/regulation of transcription - general  
5  
6    **Article type:** Research article  
7  
8    **Short title:** Zn excess induces hypoxic genes in poplar roots  
9  
10   **Corresponding author details:**  
11   Prof. Francesco Licausi  
12   Biology Department, University of Pisa, Pisa, Italy  
13   E-mail: [francesco.licausi@unipi.it](mailto:francesco.licausi@unipi.it)  
14   Phone number: +39 050 881914  
15

**Zinc excess induces a hypoxia-like response by inhibiting cysteine oxidases in poplar roots**

**Laura Dalle Carbonare<sup>1</sup>, Mark D. White<sup>2</sup>, Vinay Shukla<sup>1</sup>, Alessandra Francini<sup>1</sup>, Pierdomenico Perata<sup>1</sup>, Emily Flashman<sup>2</sup>, Luca Sebastiani<sup>1</sup> & Francesco Licausi<sup>1,3</sup>**

<sup>1</sup> PlantLab, Institute of Life Sciences, Scuola Superiore Sant'Anna, Pisa, Italy

<sup>2</sup> Department of Chemistry, University of Oxford, United Kingdom

<sup>3</sup> Biology Department, University of Pisa, Italy

**One-sentence summary:** Zinc hyperaccumulation in poplar roots simulates oxygen deficiency by inhibiting repressors of the anaerobic response

## **Footnotes**

### **List of authors contribution**

LDC, AF, LS and FL defined the aims of the project and planned the activities. LDC performed all experiments and analyzed their results. MW produced recombinant PCO proteins and, together with EF, supervised the biochemical assays. VS carried out confocal microscopy observations. LDC and FL wrote the manuscript. PP and LS critically assessed and edited the manuscript. FL agrees to serve as the author responsible for contact and ensures communication.

### **Funding information**

This work was financially supported by the PhD programme in Agrpbiosciences of the Scuola Superiore Sant'Anna (LDC, VS) and by the Biotechnology and Biological Sciences Research Council New Investigator grant BB/M024458/1 (MW and EF).

## Abstract

Poplar (*Populus* spp.) is among the tree species selected for the remediation of soil contaminated by metals, including Zn. In order to improve poplar capacity for Zn assimilation and compartmentalisation, it is necessary to understand the physiological and biochemical strategies that enable these features as well as their regulation at the molecular level. We observed an overlap between the molecular response of poplar roots to Zn excess and that activated by hypoxia. Therefore, we tested the effect of Zn excess on hypoxia-sensing components, and investigated the consequence of root hypoxia on poplar fitness and Zn accumulation capacity. Our results suggest that high intracellular Zn concentrations inhibit the activity of the oxygen sensors Plant Cysteine Oxidases, leading to the stabilisation and activation of ERF-VII transcription factors, key regulators of the molecular response to hypoxia. Remarkably, Zn excess and waterlogging similarly decreased poplar growth and development. Co-occurrence of the two stimuli did not worsen these parameters further, although it limited Zn uptake. The present study unveils the contribution of the oxygen sensing machinery to the response to Zn excess in poplar and paves the way to the exploitability of this phenomenon to improve Zn-tolerance and increase its accumulation in plants.

## Introduction

Zinc (Zn) is the second most abundant transition metal, after iron, in living organisms (Broadley *et al.*, 2007), where it is considered an essential micronutrient required to complete the life cycle. In particular, Zn is the only metal represented in all six enzyme classes - oxidoreductases, transferases, hydrolases, lyases, isomerases, ligases (Coleman, 1998; Broadley *et al.*, 2007; Bouain *et al.*, 2014), playing a structural, catalytic or co-catalytic role in more than 300 proteins (Broadley *et al.*, 2007; Ricachenevsky *et al.*, 2015). Plants acquire Zn from the soil as free  $\text{Zn}^{2+}$  whose availability depends mainly on the soil composition and pH (Bouain *et al.*, 2014). Furthermore, some plant species are able to release organic metal-chelators in the rhizosphere, in order to take the metal up more efficiently (Ricachenevsky *et al.*, 2015). From the roots, Zn is distributed to stems and leaves through the xylematic flux (Sinclair & Krämer, 2012). Although

72 Zn levels in eukaryotic cells stand in the range of 100  $\mu\text{M}$ , the concentration of free  $\text{Zn}^{2+}$  in the  
73 cytosol is usually maintained below the nanomolar range, to prevent interference with metal  
74 associated proteins (Sinclair & Krämer, 2012). This tight control of  $\text{Zn}^{2+}$  concentration is  
75 achieved through Zn high-affinity binding to phytochelatins, metallothioneins, organic acids in  
76 the cytosol and through compartmentalization of this metal into cell vacuoles (Broadley *et al.*,  
77 2007; Ricachenevsky *et al.*, 2015; Sharma *et al.*, 2016).

78 Zn concentrations above 300 ppm induce visible toxicity symptoms, including root and shoot  
79 growth impairment, leaf chlorosis and interference with P, Mg and Mn uptake (Broadley *et al.*,  
80 2007; Yadav, 2010). Zn accumulates in soils and water as a consequence of anthropogenic  
81 activities such as mining, smelting and fertilization with sewage sludge, thereby leading to Zn  
82 contamination (Broadley *et al.*, 2007; Yadav, 2010; Sinclair & Krämer, 2012; Shi *et al.*, 2015).  
83 Nowadays, phytoremediation is a cost-effective technology to clean up Zn-polluted soils,  
84 exploiting the natural capacity of some plants to absorb and transport heavy metals from the  
85 soil to the vegetative tissues (Pilon-Smits, 2005). Among plants, poplar (*Populus* spp.) is one of  
86 the most suitable species for metal phytoremediation due to its rapid growth rate, large  
87 aboveground biomass, deep root penetration and, depending on the species, the ability to  
88 accumulate a broad range of metal concentrations (Shi *et al.*, 2015). Depending on the cultivar,  
89 poplar trees are either tolerant or sensitive to the excess of heavy metals, which, in the end,  
90 influence their accumulation capacity (Pajevi *et al.*, 2016). In the present work we selected two  
91 poplar species: *Populus alba* 'Villafranca' clone, which is comparatively Zn-tolerant, and the  
92 hybrid poplar *Populus x canadensis* (*Populus deltoides*  $\times$  *P. nigra*) 'I-214' clone, which displays  
93 Zn-sensitivity (Romeo *et al.*, 2014). The phenotypic response of both varieties to Zn excess has  
94 been well characterized previously (Di Baccio *et al.*, 2003, 2005, 2009, Romeo *et al.*, 2014,  
95 2017).

96 Poplar trees thrive in several habitats from forests to riparian ecosystems (Müller *et al.*, 2013),  
97 which are regularly flooded, and therefore this tree species is considered as waterlogging and  
98 flooding tolerant (Kreuzwieser *et al.*, 2002). Flooding is typically considered as a stress factor  
99 due to the reduction of gas diffusion in water as compared with air. Indeed, a drop in oxygen  
100 levels occurs in waterlogged terrains and it is exacerbated by competitive microorganism

101 respiration (Sasidharan *et al.*, 2018). Low oxygen levels in the soil affects the development and  
 102 performance of roots, since the establishment of hypoxic conditions impairs mitochondrial  
 103 respiration, oxidation and oxygenation processes (Kreuzwieser *et al.*, 2002), and consequently  
 104 the fitness of the whole plant.

105 The response of plants to low oxygen availability has been extensively characterized and  
 106 proposed to be regulated by the concerted action of group-VII Ethylene Response Factors  
 107 (ERFs-VII) and plant cysteine oxidase (PCO) enzymes (Banti *et al.*, 2013; van Dongen & Licausi,  
 108 2015). Briefly, under normoxia, constitutively expressed ERF-VIIs are constantly degraded by  
 109 virtue of a conserved N-terminal sequence (MCGGAI) that acts as a degradation-stimulating  
 110 domain, namely N-degron (Gibbs *et al.*, 2011; Licausi *et al.*, 2011; Varshavsky, 2019). In the  
 111 presence of oxygen and nitric oxide, oxidation of the exposed cysteine in the ERF-VII degron  
 112 (Gibbs *et al.*, 2014; Weits *et al.*, 2014), generates a potential substrate for arginylation by  
 113 arginyl transferases (ATE) and subsequent polyubiquitination by the E3 Ubiquitin-ligase  
 114 PROTEOLYSIS 6 (PRT6) (Graciet & Wellmer, 2010). As a final result of these post-transcriptional  
 115 modifications, ERF-VIIs are targeted to the 26S proteasome complex to be degraded. Cysteine  
 116 oxidation is catalysed by oxygen-dependent PCOs so when oxygen availability decreases, PCO  
 117 activity is impaired and therefore the ERF-VIIs are stabilized, leading to their accumulation into  
 118 the nucleus where they regulate specific molecular responses to anaerobiosis (Gasch *et al.*,  
 119 2015; Kosmacz *et al.*, 2015). In Arabidopsis, two ERF-VII transcription factors, namely RAP2.2  
 120 and RAP2.12 have been shown to be required to activate this molecular adaptation by binding  
 121 to a conserved AAAACCA[G/C][G/C]GC DNA element defined as the Hypoxia Responsive  
 122 Promoter Element (HRPE) (Bui *et al.*, 2015; Gasch *et al.*, 2015)

123 Interestingly, floodplain wetlands, common habitats for poplars, are more often contaminated  
 124 by heavy metals than dry soils, due to increased metal availability from the soil (Abdullah,  
 125 2015). As a consequence of ore extraction and processing in particular, heavy metal residuals  
 126 are often discharged into river waters and, later on, flood events can promote remobilization of  
 127 the metals and dispersal into the surrounding areas (Ciszewski & Grygar, 2016).

128 Since flooding and metal contamination are often joint environmental cues, the possibility to  
 129 apply a plant-based remediation approach must rely on species which can adapt to both

130 conditions. In this work, we investigated the overlap of the molecular response of poplar roots  
131 to Zn excess and low oxygen conditions. By exploiting a combination of the two stresses, we  
132 elucidated the potential of this genus to cope with both conditions, from a molecular and  
133 physiological perspective, in order to evaluate its fitness and its performance in Zn  
134 accumulation.

135

136

## Results

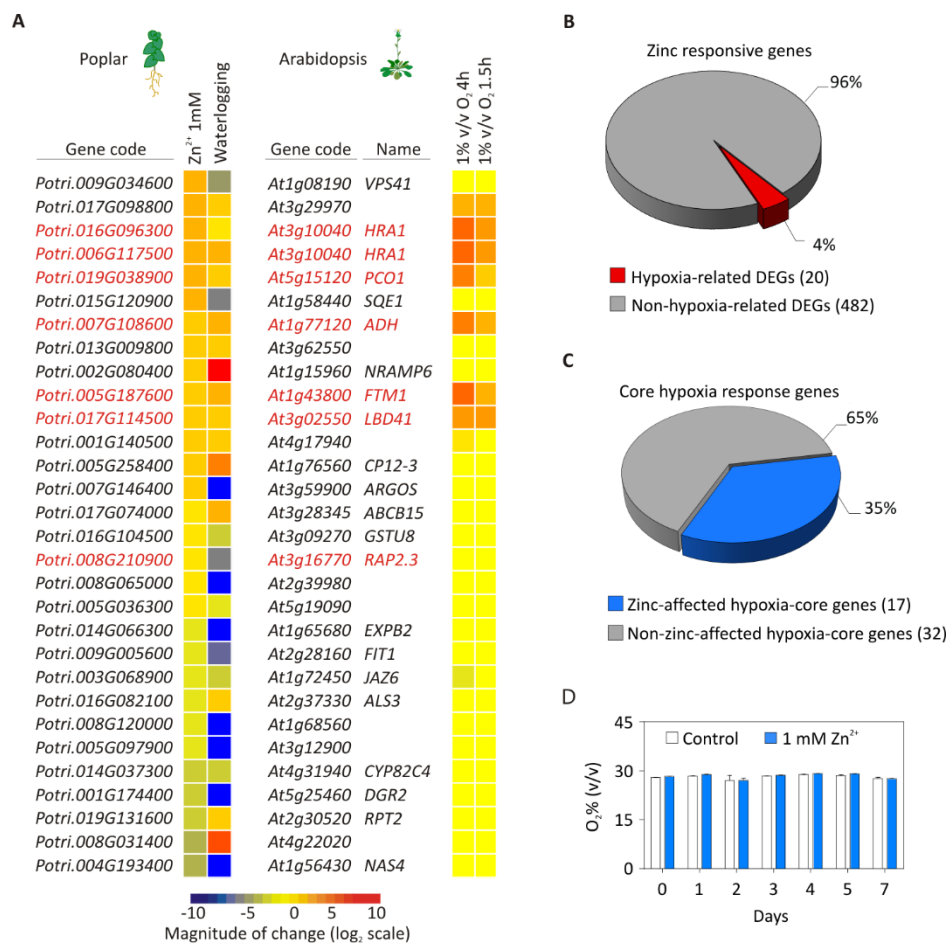
### Zn excess induces low oxygen gene responses in poplar roots

The molecular response underlying physiological sensitivity of *Populus x Canadensis* ('I-214' clone) to excess Zn has been characterized by Ariani *et al.* (2015), through a RNA-seq analysis in roots. By looking at this dataset we were struck by the apparently high occurrence of genes previously associated with the anaerobic response in different plant species. Inspired by this, we carried out a thorough comparison of the transcriptional response to Zn-stress and that of gray poplar (*Populus x canescens*) roots subjected to prolonged waterlogging (Kreuzwieser *et al.*, 2009), a condition involving insufficient oxygen provision. Thirty-nine percent of the 77 genes regulated by Zn excess were also differentially expressed in the waterlogging dataset. The expression pattern of these 30 Zn- and hypoxia-responsive genes in poplar seems to follow the same regulation as their *A. thaliana* orthologs under hypoxic conditions (Licausi *et al.*, 2010, 2011) (Fig. 1A, Supporting Table S3). In particular, the highest similarity in the transcriptional regulation pattern between poplar and Arabidopsis was observed among the up-regulated genes.

The overlap observed between the two transcriptional adaptations could still be observed by looking at a broader dataset of poplar Zn-responsive genes obtained by Ariani *et al.* (2015), applying less stringent parameters ( $\chi^2$  test, not corrected *p*-value). However, in this case, only 4% of the total Zn-related genes (20 out of 502) responded also to low oxygen conditions (Fig. 1B, Supporting Table S4).

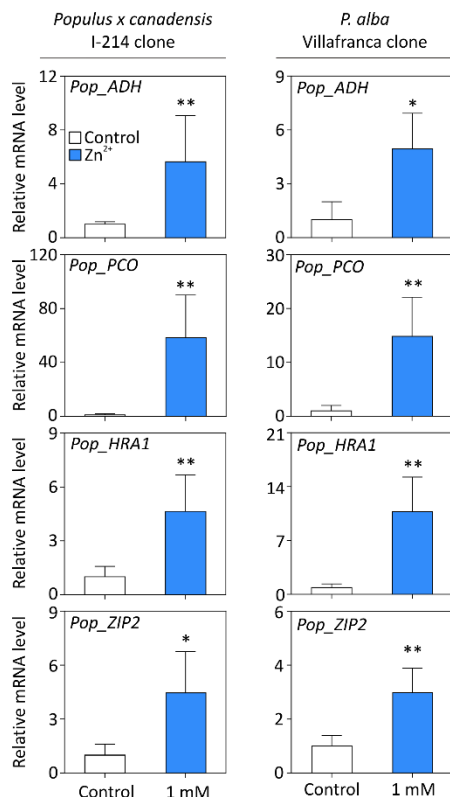
Swapping perspective, we observed that 17 (35%) genes of the 49 that constitute the core molecular response identified by Mustroph *et al.* (2009) were regulated by Zn excess in poplar (Fig. 1C, Supporting Table S5).

Considered together, these observations inspired the hypothesis that Zn excess, in addition to the activation of mechanisms dedicated to metal homeostasis and ROS scavenging (Yadav, 2010), either contributes to the reduction of oxygen availability in poplar tissues or interferes with cell signaling to elicit hypoxia-like responses at the transcript level. To address this question, we compared the oxygen concentration in the hydroponic solution where poplar plants were subjected to Zn treatment or to control conditions (Fig. 1D). The molecular oxygen



166 dissolved in the two solutions was not significantly different, suggesting that Zn treatment itself  
 167 did not increase oxygen consumption in poplar roots.



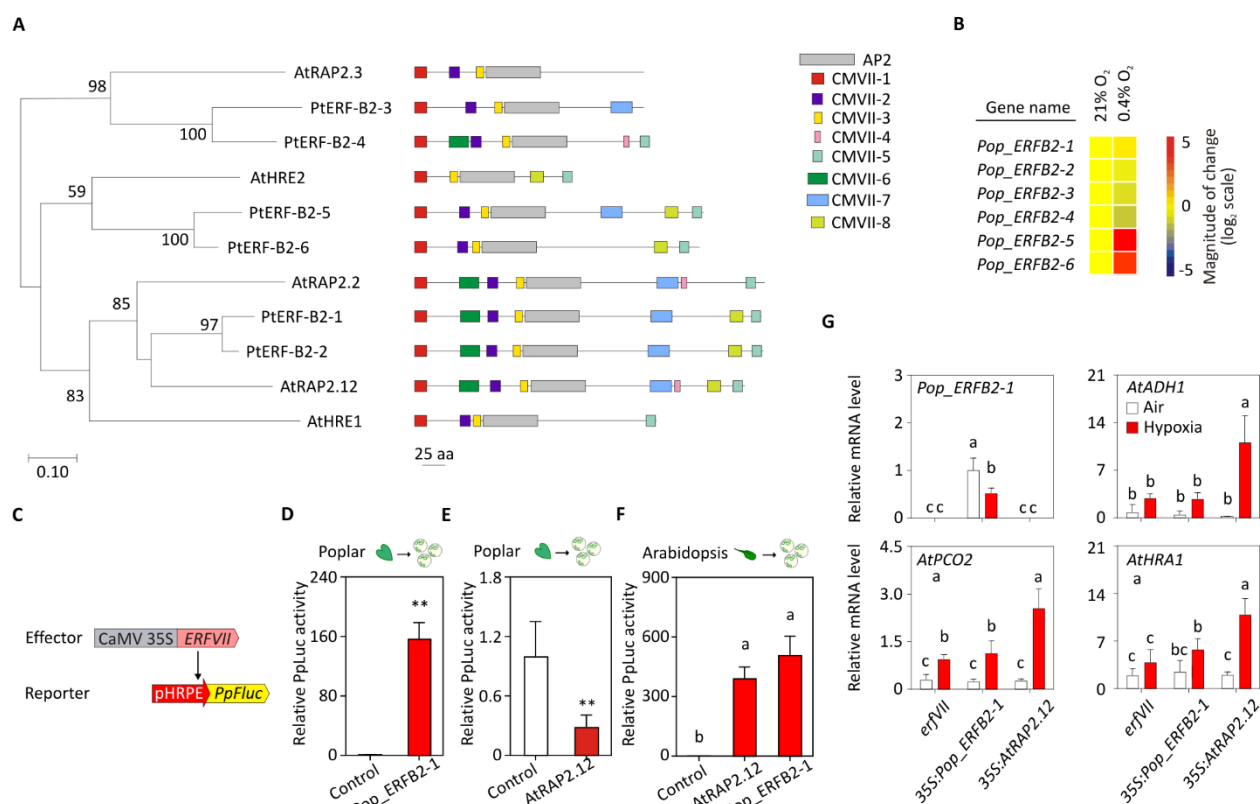


To test whether the activation of anaerobic genes under Zn stress is part of the stress symptoms manifested by these plants or is rather activated to withstand high concentrations of this metal, we compared the gene response to Zn excess in two poplar clones characterized by different tolerance extent to this stress: the *Populus x canadensis* 'I-214' used by Ariani *et al.* (2015) and *P. alba* 'Villafranca', a poplar clone characterized as Zn-tolerant (Romeo *et al.*, 2014). After 21 days of Zn treatment (1 mM ZnSO<sub>4</sub>), we observed the induction of three hypoxia marker genes *Alcohol Dehydrogenase* (*Pop\_ADH*), *Plant Cysteine Oxidase* (*Pop\_PCO*) and *Hypoxia Responsive Attenuator 1* (*Pop\_HRA1*) in the roots of both clones (Fig. 2 and Supporting Fig. 1). The induction of the Zn-stress marker gene *ZRT, IRT-like Protein 2* (*Pop\_ZIP2*), instead, confirmed the effectiveness of the treatment (Fig. 2). Since the induction of anaerobic genes did not show a clear difference between the tolerant and intolerant clones, we favored the hypothesis of poplar activating hypoxic genes as a generic response to Zn excess.

### The ERF-VII Pop\_ERFB2-1 can activate hypoxia responsive genes in poplar

Since the molecular response to low oxygen levels in *Arabidopsis* has been shown to mainly rely on the ERF-VII transcription factors RAP2.2 and RAP2.12 (ERF-VIIs) (Bui *et al.*, 2015; Gasch *et al.*,

2015), we further evaluated whether similar transcriptional regulators are responsible for the observed molecular response to hypoxia under Zn stress in poplar. A systematic comparison of the ERF-VIIs from *Arabidopsis* (Licausi *et al.*, 2010) and *P. trichocarpa* (Zhuang *et al.*, 2008) in terms of amino acid sequence occurrence and position of conserved motifs (CMVII) identified by Nakano *et al.* (2006) allowed us to identify the relatedness between different group members (Fig. **3A**). PtERFB2-1 was selected as the closest ortholog of AtRAP2.2-12, due to its high sequence similarity to the *Arabidopsis* TFs accompanied by the occurrence of eight out of nine CMVIIs (Supporting Fig. **S2**, Note **S2**). Furthermore, we assessed the transcriptional regulation of *ERF-VII* in poplar roots under anoxic conditions and observed that *Pop\_ERFB2-*



1/2/3/4 and *Pop\_ERFB2-5/6* followed the same expression pattern of *AtRAP2.2-12-3* and *HRE1-2*, respectively (Licausi *et al.*, 2010) (Fig **3B**, Supporting Table **S6**).

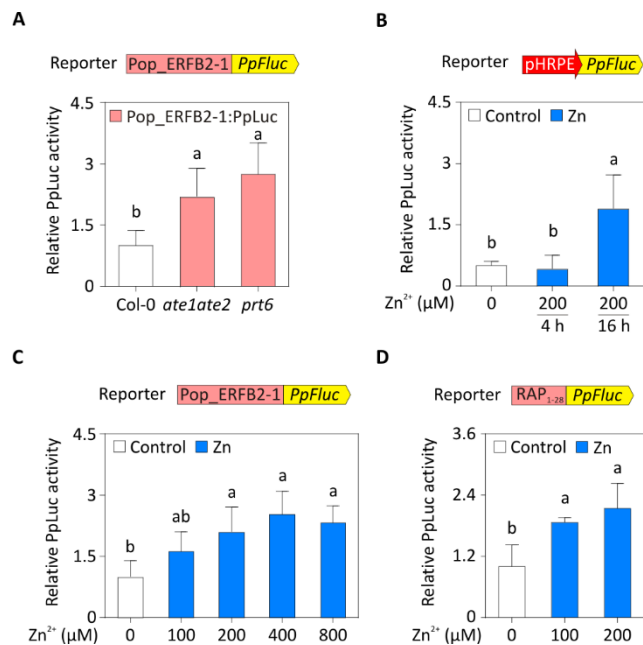
To verify whether *Pop\_ERFB2-1* can actually regulate hypoxia responsive genes in poplar, we assessed its ability to regulate a synthetic promoter bearing of a five-time repeated HRPE element (Gasch *et al.*, 2015), which was also identified in the genomic region upstream of the poplar anaerobic genes assessed before (Supporting Fig. **S3**). To this end, we transfected poplar mesophyll protoplasts with a *35S:GFP:Pop\_ERFB2-1* cassette and a reporter plasmid carrying

the 5xHRPE synthetic promoter fused to firefly *Photinus pyralis* luciferase (*PpFluc*) gene (Fig. **3c**), luminescence was measured as a readout of promoter activation. The PpFluc activity was normalized over that of sea pansy (*Renilla reniformis*) luciferase (*35S:RrLuc*) encoded by the same reporter vector. GFP:Pop\_ERFB2-1 was indeed able to strongly activate the 5xHRPE promoter in poplar protoplasts (Fig. **3D**). Remarkably, the relative luciferase activity was instead significantly reduced when a stabilized version of Arabidopsis *RAP2.12*, lacking the first 13 aa, was co-transfected with the same synthetic promoter in poplar protoplasts (Fig. **3E**). On the other hand, both stabilized forms of Pop\_ERFB2-1 and RAP2.12 could induce HRPE in Arabidopsis protoplasts (Fig. **3F**). Thus, we concluded that Pop\_ERFB2-1 is likely accountable for the induction of anaerobic genes in poplar, albeit the transactivation capacity of ERF-VII from different species relies on alternative protein partnership and regulation.

We also attempted transgenic complementation of an Arabidopsis pentuple T-DNA insertion mutant, almost entirely devoid of ERF-VII activity (Abbas *et al.*, 2015; Giuntoli *et al.*, 2017) with consequent inhibition of the transcriptional response to low oxygen conditions. Although the expression level of the *Pop\_ERFB2-1* was confirmed in four independent transgenic lines by qPCR, hypoxic genes induction after 6 h hypoxia (1% v/v O<sub>2</sub>) was not restored (Fig. **3G**). Therefore, these last results supported our hypothesis about different regulation imposed onto ERF-VIIs and their partners in poplar and Arabidopsis.

#### **Pop\_ERFB2-1 stability is enhanced by Zn in protoplasts**

Bearing in mind that Zn excess in poplar alters the expression of hypoxia-responsive genes, which are likely under control of Pop\_ERFB2-1, we further investigated whether Zn promoted the anaerobic response through Pop\_ERFB2-1. First, we measured *Pop\_ERFB2-1* expression in poplar roots subjected to Zn stress and observed that its transcriptional level did not change over the stress (Supporting Fig. **4**).



225 Similarly to other ERF-VII proteins characterized by a conserved N-terminal consensus, the  
 226 stability of Pop\_ERFB2-1 protein is expected to be controlled by the N-degron pathway. To test  
 227 this assumption, we fused the entire coding sequence of *Pop\_ERFB2-1* to *PpLuc* to generate a  
 228 post-transcriptional reporter and transfected a vector bearing this construct into Arabidopsis  
 229 protoplasts of wild type and of mutants lacking components of the N-degron pathway  
 230 (*ate1ate2* and *prt6*). Here, higher relative luciferase activity was measured in mutant  
 231 protoplasts as compared to wild type ones, suggesting increased stability of the chimeric  
 232 protein in the former cells (Fig. 4A). Consequently, we investigated whether its constitutive  
 233 proteolysis is inhibited by exposure to Zn excess using a transient transformation system based  
 234 on poplar mesophyll protoplasts. First, we verified whether ERF-VII activity is enhanced by Zn  
 235 treatment also in this system by looking at the activation of the synthetic reporter *pHRPE:PopLuc*  
 236 in the presence of 200 μM ZnSO<sub>4</sub>. Sixteen hours of Zn supplementation were necessary to  
 237 observe an increase in ERF-VII activity, whereas a short exposure to high concentrations of this  
 238 metal did not affect its expression (Fig. 4B). Next, we used the same *Pop\_ERFB2-1:PopLuc*  
 239 cassette to transfect poplar protoplasts supplemented with a range of Zn concentrations  
 240 spanning from 0 to 800 μM for 16 h (Fig. 4C). We observed a significant increase in the  
 241 luciferase activity for Zn concentrations above 100 μM showing that Pop\_ERFB2-1 protein  
 242 stability was enhanced under Zn excess in protoplasts. Comparably, a chimeric reporter,  
 243 consisting of the first 28 amino acids of AtRAP2.12 fused to the N-terminus of PpLuc, was

stabilized in Arabidopsis protoplasts treated with 100 or 200  $\mu\text{M}$  Zn for 16 h (Fig. **4D**). Thus, we concluded that the upregulation of hypoxia-responsive genes following Zn stress in poplar could be explained by the increased stability, and thereby activity, of Pop\_ERFB2-1 and possibly other poplar ERF-VIIs.

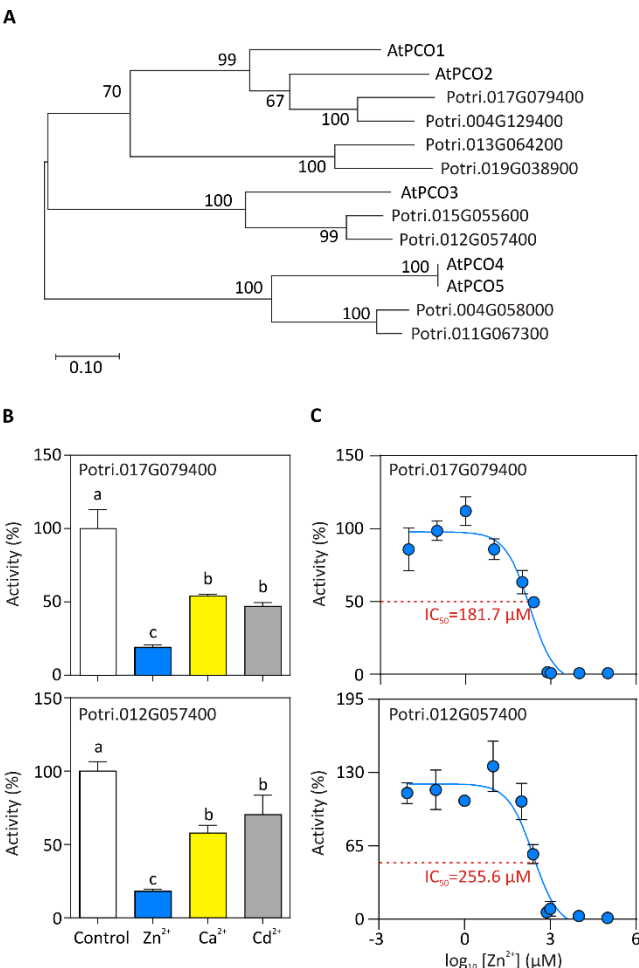
### **Zn inhibits PCO activity *in vitro***

In view of the capacity of Zn excess to cause Pop\_ERFB2-1 stabilization under aerobic conditions, we assumed that one of the steps of the N-degron pathway should be hindered by Zn itself. Among the enzymes involved in addressing ERF-VII towards proteolysis, Plant Cysteine Oxidases (PCO) are dioxygenases which catalyse the oxidation of the conserved Cys at the N terminus of the ERF-VIIs (White *et al.*, 2017). Since PCO activity seems to rely on the presence of Fe(II) in the active site (White *et al.*, 2017; White *et al.*, 2018), we hypothesized that the bivalent cation  $\text{Zn}^{2+}$  could compete with Fe(II) for the active site of the enzyme and impair its activity. We therefore used the AtPCO1 amino acids sequence as query to identify putative PCO orthologs encoded in the *P. trichocarpa* genome and found eight that clustered together their Arabidopsis counterparts to generate two main clades (Fig. **5A**, Supporting Note **S3**). We chose one poplar PCO for each cluster, Potri.017G079400 and Potri.012G057400 as closest orthologs of AtPCO1-2 and AtPCO3-4-5, respectively, and we measured their cysteine oxidation activity on a 14 aa peptide, corresponding to the N-terminus of Pop\_ERFB2-1. First, we tested *in vitro* whether the activity of the two poplar PCOs could be affected by an excess of three different cations ( $\text{Zn}^{2+}$ ,  $\text{Ca}^{2+}$  and  $\text{Cd}^{2+}$ ), dissolved in the enzymatic solution and free to access the active sites. Although all three metals could inhibit PCO activity, Zn exhibited the strongest effect (Fig. **5B**). Indeed, in the presence of 100  $\mu\text{M}$  of Zn, Potri.017G079400 and Potri.012G057400 activity was reduced by 81% and 82%, respectively. We also evaluated the extent of such inhibition, in terms of  $\text{IC}_{50}$  values (Fig. **5C**). We measured the activity of the enzymes in the presence of a wide range of Zn concentrations from 10 nM to 100 mM, compared to control conditions (100% of activity). For both Potri.017G079400 and Potri.012G057400, the  $\text{IC}_{50}$  values were comparable at 181.7 and 255.6  $\mu\text{M}$ , respectively. We therefore favoured the hypothesis that Zn excess

272 promotes ERF-VII stabilization and the consequent induction of anaerobic genes by inhibiting  
273 the oxidase enzymes that targets these proteins to proteasomal degradation.

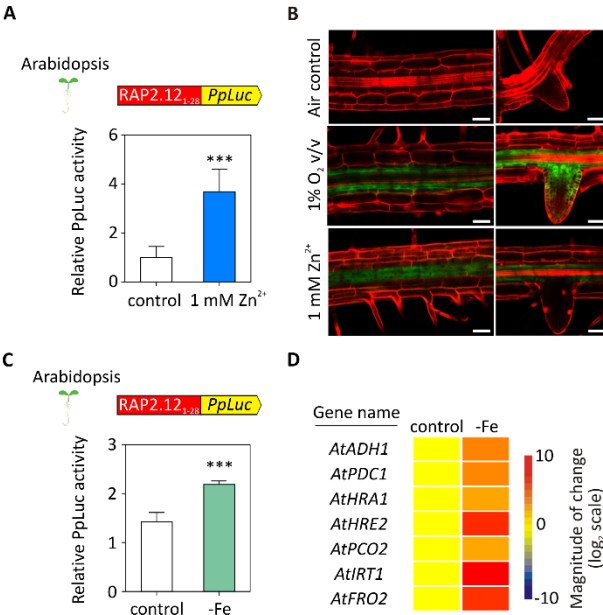
274 **Zn excess mimics Fe deficiency to induce hypoxia-responsive genes**

Several genes involved in iron deficiency signaling and homeostasis, such as *Natural Resistance Associated Macrophage Protein 1 and 6 (NRAMP1 and 6)*, *bHLH038* and *Zig Suppressor 2 (ZIP2)* (Ariani *et al.*, 2015), responded to Zn stress in poplar (Fig. 1A). Since PCOs require Fe<sup>2+</sup> to



oxidize N-terminal cysteine (White *et al.*, 2018), we speculated that Zn excess may mimic iron starvation *in vivo* in terms of ERF-VII transcription factors. To test this hypothesis, we generated transgenic Arabidopsis plants that express the *RAP2.12<sub>1-28</sub>-PpLuc* construct under the control of the 35S CaMV promoter. Firefly luciferase activity was significantly stimulated in five-day old seedlings treated with 1 mM Zn for 72 h (Fig. 6A), confirming the results obtained with transiently transformed protoplasts (Fig. 4D). Moreover, Zn stress and hypoxia (1% O<sub>2</sub> v/v) exhibited the same inductive effect on the synthetic promoter *pHRPE* (Weits *et al.*) in the roots of 10 days old plants (Fig. 6B). Next, we tested whether iron starvation could stabilize ERF-VII proteins and indeed measured higher luciferase in iron starved *RAP2.12<sub>1-28</sub>-PpLuc* seedlings as

compared to iron fed ones (Fig. 6C). Additionally, iron deficiency also induced higher expression of several hypoxia-responsive genes (Fig. 6D, Supporting Table S7). Considered together, these results supported the hypothesis that ERF-VII are stabilized when PCOs are inhibited by



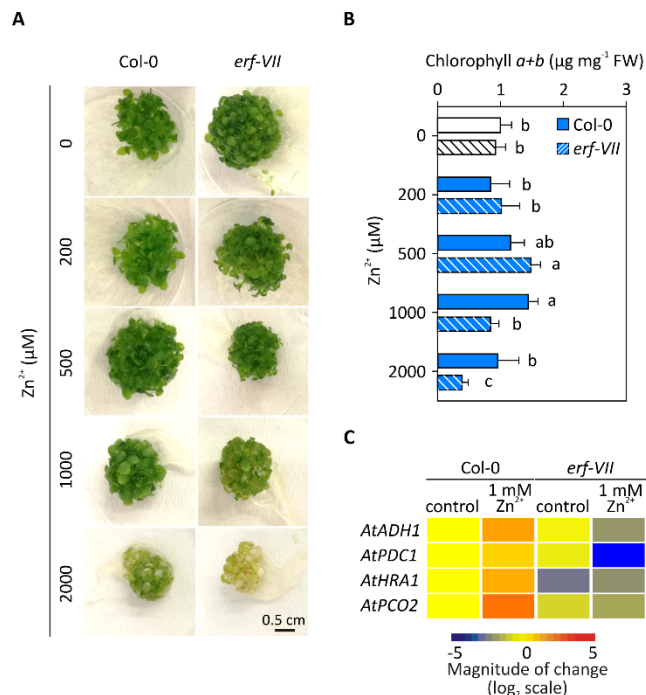
substrate (O<sub>2</sub>) or by co-factor (Fe<sup>2+</sup>) shortage, the latter being caused by actual low iron levels or Zn competition.

### ERF-VII responsive genes improve tolerance to Zn excess in Arabidopsis

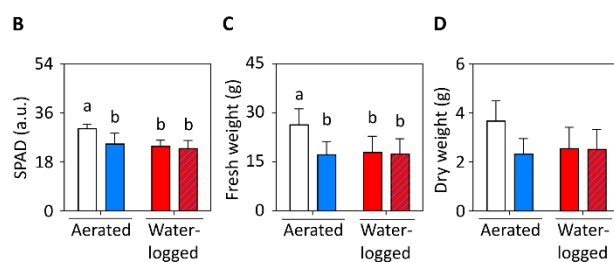
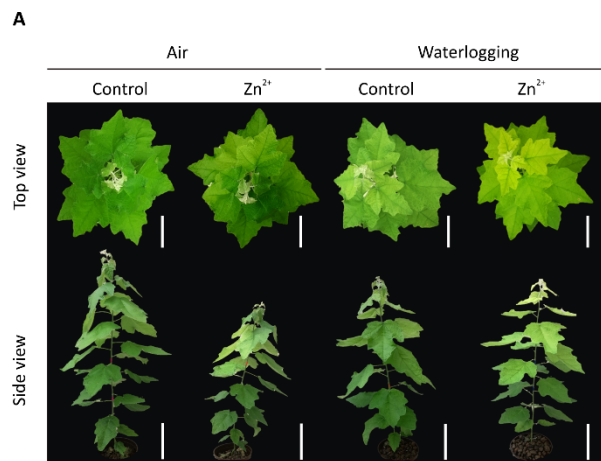
Once observed that Zn excess or iron starvation enhance the expression of hypoxia-responsive genes through inhibiting PCO in poplar and Arabidopsis, we wondered whether ERF-VII activity provide protection against Zn stress. Thus, we compared *erf-VII* mutant seedlings and wild-type ones after three days of Zn supplementation at different concentrations. Remarkably, this mutant exhibited higher sensitivity to Zn, as also demonstrated by reduced growth and total chlorophyll accumulation (Fig. 7A and B), accompanied by reduced expression of ERF-VII genes by Zn excess in the *erf-VII* genotype (Fig. 7C, Supporting Table S8). These results support the idea that induction of hypoxia-responsive genes by ERF-VII also contribute to Zn tolerance, at least in Arabidopsis.

### Zn stress and waterlogging affect poplars fitness





Poplar trees can be used for phytoremediation of heavy metals in riparian areas, which are regularly subjected to flood events since they are able to grow in waterlogged, and thereby hypoxic, soils (Isebrands & Richardson, 2014; Ciszewski & Grygar, 2016). Considering the molecular cross-talk between Zn excess and hypoxia in this species, we were interested in monitoring the plant physiological response and fitness under the combination of Zn stress and waterlogging. We therefore subjected *P. alba* 'Villafranca' poplar plants to four different hydroponic conditions: aerated control solution, Zn excess (1 mM ZnSO<sub>4</sub>), waterlogging and a combination of the two stresses, for 4 and 10 days. After 4 days, plants did not show any significant difference in terms of fresh and dry biomass, as compared to the control condition (Supporting Tables S9 and S10).

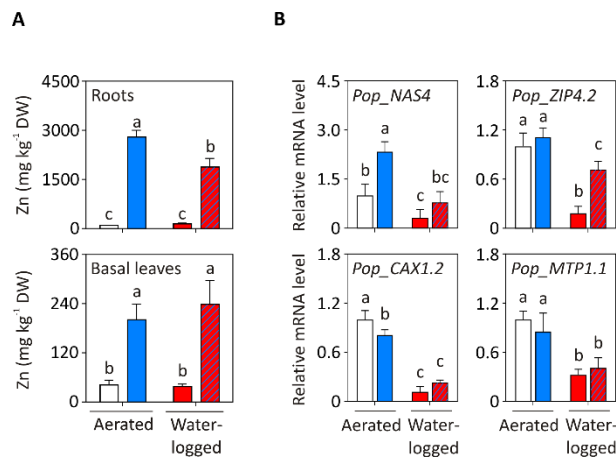


Instead, after 10 days of growth in the conditions described above, Zn-stressed and waterlogged plants displayed a similar symptomatic phenotype, when compared to the controls: they both showed chlorosis in the younger leaves and reduced growth (Fig. 8A). We therefore quantified the chlorotic phenotype in terms of total chlorophyll content (SPAD units), resulting in a significant decrease of the chlorophyll in all three stress conditions, as compared to the control (Fig. 8B). Ten days of treatment caused a decrease in total biomass compared to the controls, as shown by a significant decrease in fresh weight (Fig. 8C, Supporting Table S11), followed by the same trend in dry weight, even though not significant (Fig. 8D, Supporting Table S12).

These results prompted us towards two main speculations. First, both Zn excess and waterlogging exert a similar repressive effect on poplar growth and thereby possibly impact on similar molecular mechanisms. Moreover, since the combination of the two stresses did not impair biomass production and chlorophyll accumulation more than each single treatment, the reduction in growth rate could be considered as an adaptive strategy to cope with unfavorable environmental conditions.

### Waterlogging affects Zn accumulation in poplar roots

Once established that root hypoxia and Zn excess share similarities in their phenotypic adaptations as well as in the molecular response, we tested whether waterlogging may impact on Zn accumulation and thereby affect the performance of the Zn tolerant poplar ‘Villafranca’ clone in phytoremediation. Leaves and root tissues were collected from plants subjected to the growth conditions described in the previous paragraph to evaluate their Zn content. As expected from the phenotypes described above (Fig. 8), substantial Zn accumulation occurred after 10 days in plants subjected to Zn treatment both under aerated and waterlogged conditions (Fig. 9). However, we recorded a significant reduction of Zn levels in the roots of Zn-treated plants when these were also subjected to waterlogging, as compared to the metal supplementation under aerated conditions. Surprisingly, such effect of waterlogging on Zn accumulation was not detected in the leaves (Fig. 9A), despite the likely occurrence of ATP shortage under waterlogging (Gibbs & Greenway, 2003), which would have been expected to impact on the active loading of Zn into the xylem and thereby on its distribution to the shoot (Olsen & Palmgren, 2014). Nevertheless, in agreement with the reduced radical accumulation of Zn, we detected a significant reduction in the expression of genes involved in metal acquisition and transport in root tissues under waterlogged conditions (Fig. 9B, Supporting Table S13). Among these, *Nicotianamine Synthase 4* (*Pop\_NAS4*) contributes to the production of non-proteinogenic amino acid that chelates cations to facilitate their uptake in the roots and their translocation through the vessels (Schuler & Bauer, 2011; Open *et al.*, 2014). On the other hand, *Pop\_ZIP4.2* encodes for a membrane Zn transporter, while *Pop\_CAX1.2* and *Pop\_MTP1.1* for two vacuolar Zn-H<sup>+</sup> antiporters. We speculated that, under waterlogging, the plants reduced root Zn accumulation by decreasing the Zn uptake (via *Pop\_ZIP4.2* and NA-chelation) and limiting its compartmentalization into the vacuole (via *Pop\_CAX1.2* and *Pop\_MTP1.1*). Taken together, these results suggested that poplar can tune Zn uptake in the root to cope with unfavorable soil conditions, such as waterlogging.



## Discussion

In this work, we investigated the convergence of molecular and physiological responses of poplar trees to Zn excess and waterlogging, and proceeded to examine the adaptation to the combination of these two stresses. So far, this aspect has remained overlooked, despite its relevance for soil Zn remediation and poplar physiology. Indeed, the recently increased frequency of flooding events intensifies the probability that contaminants, including metals, are remobilized from the rivers banks to the surrounding riparian areas (Ciszewski & Grygar, 2016). For this reason, phytoremediation of these areas has focused on employing plants species that thrive in naturally flooded areas and tolerate high amount of metals, such as poplars (Pilon-Smits, 2005; Müller *et al.*, 2013).

By comparing the transcriptional responses of poplar roots to Zn stress (Ariani *et al.*, 2015) and waterlogging (Kreuzwieser *et al.*, 2009), we observed a remarkable overlap between Zn-regulated genes and hypoxia-responsive ones. The hypoxia-like response activated under Zn stress appeared to be part of the adaptive response of the plants to Zn stress, rather than being induced by an actual reduction in oxygen availability in the roots, in response to Zn excess (Fig. 1). The similarity between these responses was conserved irrespectively of the Zn tolerance of the poplar variety, as demonstrated by its occurrence in two poplars cultivars characterized by different sensitivity to Zn stress (Fig. 2) (Romeo *et al.*, 2014).

In *Arabidopsis*, the transcriptional response to hypoxia is regulated mainly by the ERF-VII transcription factors RAP2.2 and RAP2.12, whose aerobic instability is ensured by the N-degron pathway (van Dongen & Licausi, 2015). Additional control by light, potassium and sugar

availability has been reported to impact on the stability and activity of these proteins (Abbas *et al.*, 2015; Shahzad *et al.*, 2016; Loreti *et al.*, 2018). Unbalanced metal homeostasis is likely to affect, directly or indirectly with these regulatory pathways. In this study, we focused on the control exerted by PCOs, responsible for the oxidation of the Cys in second position of the ERF-VII that precedes their degradation (Weits *et al.*, 2014). PCOs were recently shown to require molecular oxygen and  $\text{Fe}^{2+}$  to oxidase the Cys (White *et al.*, 2017, 2018). Interestingly, we observed that, *in vitro*, divalent cations were able to inhibit the enzyme activity and  $\text{Zn}^{2+}$  was especially effective at it (Fig. 5). We therefore speculated that  $\text{Zn}^{2+}$  may also outcompete  $\text{Fe}^{2+}$  for PCO binding *in vivo*. Indeed, prolonged iron starvation also caused stabilization of an ERF-VII reporter and induced hypoxia responsive genes in Arabidopsis seedlings (Fig. 6C and D). This is in agreement with the transcriptional response of Arabidopsis roots to two days of iron limitation reported by Dinneny *et al.* (2008). The very high Zn concentrations required for PCO inactivation *in vitro*, in the micromolar range, induced us to question the physiological relevance of this phenomenon. On the one hand, the activity of other enzymes, such as Carboxipeptidase A and Kallikreins, has been shown to be inhibited at similar metal concentrations (Maret, 2013). On the other hand, cytosolic and nuclear Zn levels of poplar root cells exposed to Zn excess in the soil are still unknown. Pioneering endeavors in assessing subcellular  $\text{Zn}^{2+}$  levels through a genetically encoded FRET-based sensor have been conducted using Arabidopsis root cells, although the saturation of the sensor did not allow the detection of Zn concentrations above the nanomolar range (Lanquar *et al.*, 2014). However, in balanced nutrient conditions, Arabidopsis mesophyll vacuoles contain Zn in the micromolar range (Lanquar *et al.*, 2010). Considering soil Zn content reaches up to thousands  $\text{mg kg}^{-1}$  levels in contaminated soils (Long *et al.*, 2003), it is not unlikely that the intracellular concentration of this metal in root cells may reach the concentrations compatible with PCO inhibition. It is also worth considering that long time exposure to Zn excess was necessary to activate the hypoxia-like response in poplar roots, since Zn supplementation for four hours was unable to activate the ERF-VII reporter in protoplasts (Fig. 4). We therefore speculate that PCO enzymes might be especially sensitive to Zn inactivation during their biogenesis at the time when the metal ion is

incorporated. During chronic exposure to Zn excess, such as in our experimental conditions, this would lead to the accumulation of inactive PCOs over time.

Despite acting as a cofactor or structuring element for several proteins,  $\text{Zn}^{2+}$  represents a threat for many iron-containing enzymes. Indeed, among biogenic metal species characterized by positive divalent charge and ionic radius similar to iron, Zn possesses higher ligand coordinating strength according to the Irving-Williams series (Irving & Williams, 1948) and is therefore likely to form more stable complexes. In light of this, despite metalloproteins having evolved to preferentially accommodate the cognate cation that ensures their biological function and to protect the binding sites from the attack of undesired metal contenders, Zn can easily displace and substitute iron (Dudev & Nikolova, 2016). It is therefore responsibility of the cell machinery to maintain Zn homeostasis to levels that prevent competition with  $\text{Fe}^{2+}$ . In this perspective, the inactivation of poplar PCO enzymes at cellular Zn concentrations below or in the proximity of toxic levels, as demonstrated by the survival and limited reduction in the growth rate (Fig. 8), is surprising: this specific molecular mechanism is rather Zn-sensitive for a plant species able to accumulate high intracellular Zn levels (Sebastiani *et al.*, 2014). Thus, we speculated that this enzymatic sensitivity to moderate Zn levels might rather have a signaling function in poplar, via ERF-VIIs or other transcription factors controlled by the N-degron pathway.

Induction of ERF-VII-regulated genes appeared to be beneficial for tolerance to Zn excess in Arabidopsis (Fig. 7A-C). Future studies should be aimed at understanding whether the whole anaerobic response is required for Zn tolerance or if some genes play a major role.

Additional mechanisms may be activated by Zn or low iron-induced inactivation of PCOs. Four bHLH TFs, namely bHLH38/39/100/101, have been identified as being involved in iron sensing in Arabidopsis (Sivitz *et al.*, 2012). All four bHLHs are characterized by a conserved Cys residue in the penultimate position that makes them potential N-degron substrates. Poplar orthologs of these genes are also transcriptionally up-regulated in response to Zn excess, suggesting their potential involvement in the adaptive response to this stress (Ariani *et al.*, 2015). Future experimental efforts may be aimed at addressing whether post-translational stabilization via PCO inhibition is involved in the induction of their activity. Moreover, the involvement of MC-

437 proteins in the response to Zn excess and iron-deficiency might suggest a common evolution of  
438 nutrient homeostasis mechanisms that over time diverged into the ERF-VII and bHLHs families.  
439 As mentioned before, the inhibition of PCO activity under limiting oxygen conditions has been  
440 associated with the up-regulation of hypoxia-related genes via the stabilization of ERF-VII  
441 (Weits *et al.*, 2014). Here, we observed that the Pop\_ERFB2-1, a close RAP2.12/2 ortholog in  
442 poplar, is able to activate hypoxia-responsive genes (Fig. 3). In agreement with the proposed  
443 inactivation of PCO activity by Zn, this transcription factor can be stabilized by Zn excess at  
444 normoxic oxygen levels (Fig. 4). Despite the high sequence similarity between RAP2.12 and  
445 Pop\_ERFB2-1, the latter failed to restore the molecular response to anaerobiosis in the  
446 Arabidopsis pentuple *erf-VII* mutant (Fig. 3). This could be explained by small differences in the  
447 amino acid sequences between the two ERF-VIIs that hindered or altered the interaction of  
448 Pop\_ERFB2-1 with the Arabidopsis ERF-VII partners that enable recruitment of the  
449 transcriptional complex on the promoters of target genes. Moreover, RAP2.12 was unable to  
450 activate anaerobic genes when transiently expressed in poplar protoplasts (Fig. 3E). Previous  
451 protein-interaction surveys identified ERF-VII interactors involved in transcriptional regulation  
452 in Arabidopsis: RAP2.2 was shown to bind to the Mediator complex subunit Med25, which likely  
453 serves as a scaffold for the assembly of RNA polymerase II and general transcription factors,  
454 and the chromatin-remodeling ATPase BRAHMA (Ou *et al.*, 2011; Vicente *et al.*, 2017).  
455 Additionally, interaction with transcription factors belonging to different protein families, and  
456 which may mediate binding to additional targets under specific conditions, were also reported  
457 (Lumba *et al.*, 2014). The failure in complementing the light-sensing negative regulator *spa*  
458 Arabidopsis mutant by PpSPAb or OsSPA1, from *P. patens* and *O. sativa* respectively (Ranjan *et al.*  
459 *et al.*, 2014) is another example of the interactors specificity required for a TF to exert its function.  
460 The overlap between the transcriptional response to Zn and low oxygen observed in poplar is of  
461 great interest since these species are not unlikely to experience a combination of these two  
462 stresses, for the reasons mentioned above. Remarkably, ten days of 1 mM Zn supplementation  
463 or waterlogging exerted a similar effect on the tolerant *P. alba* 'Villafranca'. Both treatments  
464 reduced biomass accumulation and with concomitant chlorosis of the younger leaves (Fig. 8).  
465 The apparent discrepancy with the previously reported absence of toxicity symptoms in the

'Villafranca' plants exposed to 1 mM Zn (Romeo *et al.*, 2014) is likely explained by the different anion used in our experimental conditions: ZnSO<sub>4</sub> instead of Zn(NO<sub>3</sub>)<sub>2</sub>. Additionally, we put forward two explanations for the observed toxic effect of Zn. First, this metal could compete with iron to be taken up in the roots via low-affinity transporters, such as IRT1 (Sinclair & Krämer, 2012). Consequently, Zn-induced iron starvation might repress chlorophyll biosynthesis, since heme synthesis requires iron and Zn is likely to replace Mg<sup>2+</sup> in the porphyrin ring (Tripathy & Pattanayak, 2012). Alternatively, stabilized ERF-VII proteins, induced by either Zn excess or waterlogging, could be involved in active repression of chlorophyll biosynthetic genes as reported by Abbas *et al.* (2015).

Since the combination of Zn excess and waterlogging did not enhance leaf chlorosis and biomass reduction as compared to the single stresses (Fig. 8), we concluded that the two environmental cues impact to the same extent on these regulatory and biosynthetic pathways. Instead, we observed a decrease in Zn accumulation in poplar roots under Zn stress and waterlogging, compared to Zn excess, concomitant with the repression of genes involved in Zn uptake and vacuolar compartmentalization (Fig. 9). This can be interpreted as a conservative strategy to limit Zn accumulation before it reaches toxic cellular concentrations when the plant metabolism is already dedicated to coping with oxygen deficiency at the root level.

In conclusion, in this work we shed new light on the cross-talk in the molecular and physiological response of poplars to two environmental stresses: Zn excess and waterlogging. In a phytoremediation perspective, understanding the adaptive responses of plants to this specific combination of environmental cues is fundamental to identify agronomic practices and breeding strategies that will make this approach more effective, reliable and widely applicable.

## Materials and Methods

### Plant material and growth conditions

Plantlets of *Populus alba* L. 'Villafranca' clone were maintained *in vitro* conditions in Magenta™ vessels on 0.7% (w/v) agar woody plant medium (WPM) at pH 5.7 (Lloyd and McCown, 1980). Four weeks-old plantlets, derived from *in vitro* culture (half-strength WPM medium), were transferred to pots filled with perlite (Laterlite), and closed in plexiglass boxes to maintain the



100 % humidity. The plantlets were acclimatized for 4 weeks under controlled environmental conditions (23:18 °C day:night temperature, 65–70 % relative humidity, and 16 h photoperiod, at photosynthetic photon flux density of 400  $\mu\text{mol m}^{-2} \text{s}^{-1}$  supplied by fluorescent lights). Hoagland's solution (Arnon and Hoagland, 1940) was supplied as a nutrient solution and relative humidity was gradually reduced from 100 to 65–70 %. After the acclimation period, plants were transferred into plastic pots containing 4–8  $\varnothing$  mm expanded Agrileca clay (Laterlite) and grown in Hoagland solution with continuous aeration by aquarium pumps (250 L h<sup>-1</sup>).

Woody cuttings of 'Villafranca' and *Populus x canadensis* 'I-214' clone were provided by Centro di Ricerche Agro-Ambientali 'Enrico Avanzi' CiRAA (Pisa, Italy). After rooting, cuttings were transferred into plastic pots, containing 4–8  $\varnothing$  mm expanded Agrileca clay (Laterlite), and acclimated to a hydroponic system under controlled environmental conditions, as described before. At the end of the acclimation process, plants were pruned and maintained at unique stem growth.

Seeds of the *Arabidopsis erf-VII* mutant, described in Abbas *et al.* (2015), have been provided by Michael Holdsworth. Seeds of *prt6-5* (SALK\_051088) and *ate1ate2* mutants have been previously described by Gibbs *et al.* (2011) and Licausi *et al.* (2011), respectively. Columbia-0 (Col-0) ecotype was used as a wild-type reference. *Arabidopsis thaliana* seeds were sown in moist soil, stratified at 4 °C in the dark for 48 h and germinated at 22:18 °C day:night with 16 h photoperiod. For *in vitro* seedlings cultivation, seeds were sterilized and, subsequently, germinated in 2 ml liquid half-strength MS (Murashige & Skoog, 1962) medium supplemented with 1% (w/v) sucrose (Duchefa), in 6-wells plates (Euroclone), under 90 rpm shaking.

### **Cloning of the various constructs**

The full coding sequence (cds) of the closest *Arabidopsis RAP2.12* gene (*At1g53910*) homolog in poplar (*Potri.003G071700*, named *PtERFB2-1*, according to Zhuang *et al.*, 2008) has been cloned from *P. alba* 'Villafranca', using Phusion High Fidelity DNA-Polymerase (New England Biolabs) with primers designed on *P. trichocarpa* genome. The high similarity between 'Villafranca' (*Pop\_ERFB2-1*) and *P. trichocarpa* (*PtERFB2-1*) sequences at the nucleotide and amino acid levels are shown in Supporting Note S1.

*Pop\_ERFB2-1* amplicon was cloned into *pENTR/D-TOPO* (Life Technologies), and then recombined into *p2GW7*, *p2GWL7* and *pGWB514* (Life Technologies) destination vectors using the LR reaction mix II (Life Technologies).

The cds of two 'Villafranca' poplar *PCOs* (*Potri.012g057400* and *Potri.017g079400*) were isolated using primers designed on *P. trichocarpa* genome and carrying *NdeI* and *XhoI* sites at the 5' of forward and reverse primers, respectively. The *NdeI/XhoI* fragments were ligated into *pET28a(+)* vector, suitable for protein expression and purification through a N-term His<sub>6</sub>-tag. All the primers used for cloning of the described fragments are listed in Supporting Table **S1**.

### **Luciferase transactivation and protein stability assay**

'I-214' mesophyll protoplasts were isolated and transfected according to Yoo *et al.* (2007). Two micrograms and a half of each plasmid was used to transfect 100 µL of protoplasts suspension. After over-night incubation in the dark at 23 °C, the firefly (*Photinus pyralis*) luciferase was measured and normalized with the *Renilla* luciferase signal (PpLuc/RrLuc), using the Dual-Luciferase<sup>®</sup> Reporter (DLR<sup>™</sup>) Assay System (Promega), according to the manufacturer's protocol. For each sample, five independent replicates were used.

### **Low oxygen and Zn treatments**

After 10 days of hydroponic solution, woody cuttings of poplar plants were randomized in groups of five plants and subjected to the following treatments. 'Villafranca' and 'I-214' cuttings were treated with 1 mM ZnSO<sub>4</sub> (1 µM as control) for 21 days. The total amount of ZnSO<sub>4</sub> given in 21 days was 0.78 g per plant. 'Villafranca' poplars acclimated *in vitro*, instead, were treated with 1 mM ZnSO<sub>4</sub> (1 µM as control), waterlogging and a combination of the two stresses for 4 or 10 days. The total amount of ZnSO<sub>4</sub> given in 10 days was 0.43 g per plant.

Poplar mesophyll protoplasts were incubated with different concentrations of ZnSO<sub>4</sub> (0, 100, 200, 400, 800 µM), dissolved in the WI solution (0.5 mM mannitol, 4 mM MES-KOH at pH 5.7, 20 mM KCl), over-night.

Four-day-old Arabidopsis seedlings were subjected to a 6 h partial submergence treatment provided by an addition of 3 ml of fresh half-strength MS (1 % sucrose), in the dark, to avoid

oxygen release by photosynthesis, without shaking. Control seedlings were kept in the dark, under shaking conditions.

Five-day-old *Arabidopsis* seedlings cultivated on liquid half-strength MS, supplemented with 1 % sucrose (w/v), were transferred to control medium (0  $\mu$ M of  $\text{ZnSO}_4$ ) or to medium supplemented with  $\text{ZnSO}_4$  (200, 500, 1000 or 2000  $\mu$ M) for three days.

For confocal microscopy observations, seven-day-old *Arabidopsis* seedlings were grown on square plastic plates (12 cm side) containing 50 mL of half-strength MS, supplemented with 1 % sucrose (w/v), and 0.8% (w/v) of plant agar. Subsequently plates were treated with 1%  $\text{O}_2$  (v/v) for 6 h or with 1 mM  $\text{ZnSO}_4$ , dripped on the root surface, for 48 h.

#### **Germination under iron starvation conditions**

*Arabidopsis* seeds were germinated and grown for six days under control (half-strength MS containing 50  $\mu$ M of FeNaEDTA and supplemented with 1 % (w/v) sucrose) or iron-devoid (half-strength MS, 0  $\mu$ M FeNaEDTA and 1 % sucrose) conditions.

#### **Oxygen measurement**

Molecular oxygen measurements in hydroponic solution were performed through the optical oxygen meter FireStingO2 (PyroScience), using the OXF500PT fiber-optic micro sensor, according to the manufacturer's protocol.

#### **Chlorophyll quantification**

The relative chlorophyll concentrations were estimated using a SPAD-502 chlorophyll meter (Minolta), on ten fully expanded 'Villafranca' poplar leaves randomly selected among the four treatments after 10 days of the Zn and waterlogging combined experiment.

Eight-day-old Col-0 and *erf-VII* *Arabidopsis* seedlings were frozen, grinded and the resulting powder was incubated with 100% v/v methanol overnight at 4°C in the dark. After centrifugation, the supernatant was separated from the pellet and the absorbance of the extract was spectrophotometrically measured at 665.2 and 652.4 nm. Chlorophyll concentrations were calculated according to Lichtenthaler's (Lichtenthaler, 1987).

### **Zn concentration analysis in poplar**

The total concentration of Zn in poplar dry roots and leaf, after 4 or 10 days, was determined after digestion with concentrated nitric acid (HNO<sub>3</sub>) by atomic absorption spectrophotometry (model 373, PerkinElmer). One analytical reference standard of Zn was used as a control (WEPAL IPE, Wageningen University).

### **Plant transformation and genotyping**

*Arabidopsis erf-VII* stable transgenic plants were obtained using the floral dip method (Clough & Bent, 1998). T<sub>0</sub> seeds were screened for hygromycin resistance; two independent transgenic lines were identified (35S:*Pop\_ERFB2-1* line #2 and #3) and the presence of *Pop\_ERFB2-1* cDNA was tested via PCR using a GoTaq® DNA polymerase (Promega) using the primers listed in Supporting Table S1.

### **Identification of poplar PCOs**

Identification of PCO protein sequences in *P. trichocarpa* was performed by searching the Phytozome database (www.phytozome.net), using the BLAST algorithm (Altschul *et al.*, 1990) and *Arabidopsis* PCO1 (At5g15120) as a query. The obtained proteins were then aligned back against the *A. thaliana* protein database to ensure that they represent the closest homologs of AtPCOs.

### **Phylogenetic analysis**

Phylogenetic analysis was performed using MEGAX (Kumar *et al.*, 2018). The phylogenetic trees were obtained aligning *Arabidopsis* and poplar PCOs and ERF-VIIs using the MUSCLE algorithm (Edgar, 2004). The maximum-likelihood method was applied to build the phylogenetic trees, using a bootstrapping method based on 100 replicates.

### **PCO purification and *in vitro* inhibition assay**

610 *P. alba* 'Villafranca' PCOs (Potri.012g057400 and Potri.017g079400) were purified using Ni<sup>++</sup>  
611 affinity chromatography, following the protocol described in (White *et al.*, 2018). Cysteine  
612 oxidation activity of PCOs was measured towards a 14 aa peptide (ERFB2-1<sub>2-16</sub>, H<sub>2</sub>N-  
613 CGGAIISDFIAPTT-COOH), corresponding to the N-terminus of PtERFB2-1 protein  
614 (Potri.003G071700). The metal inhibition assays were performed in 30 µl buffer: 20 mM NaCl,  
615 20 mM 4-(2-hydroxyethyl)-1-piperazineethanesulfonic acid (HEPES), 1 mM TCEP (tris(2-  
616 carboxyethyl)phosphine) and 1 mM L-ascorbic acid, at pH 7.5. Buffer was supplemented with  
617 25 nM of enzyme, 1 mM of substrate and 1 mM of inhibitor (ZnCl<sub>2</sub>, CaCl<sub>2</sub> or CdCl<sub>2</sub>). The  
618 reactions were run for 1.5 min at 25 °C and stopped by quenching 5 µl in 45 µl of 1 % formic  
619 acid.

620 For the Zn IC<sub>50</sub> assays, a wide range of Zn<sup>2+</sup> (ZnCl<sub>2</sub>) concentrations (10 nM, 100 nM, 1 µM, 10  
621 µM, 100 µM, 250 µM, 750 µM, 1 mM, 10 mM and 100 mM) were tested. The enzymes were  
622 incubated on ice with the metal for 30 min before performing the reactions for 2 min. All the  
623 samples were analysed by HPLC chromatography coupled with quadrupole-TOF mass  
624 spectrometry (Xevo® G2-XS QToF) as previously described by White *et al.* (2018).

625

#### 626 **RNA extraction and qRT-PCR analysis**

627 Poplar total RNA was isolated from 80-100 mg of frozen and grinded roots using Spectrum™  
628 Plant Total RNA Kit (Sigma-Aldrich), according to the manufacturer's protocol.

629 For *Arabidopsis* RNA extraction, a phenol-chloroform extraction protocol was employed, as  
630 described in Weits *et al.* (2014). One microgram of RNA was subjected to DNase treatment  
631 along with cDNA synthesis, both performed with Maxima First Strand cDNA Synthesis Kit for RT-  
632 qPCR with dsDNase (Thermo Scientific).

633 Quantitative real-time PCR amplification (qRT-PCR) was carried out with the ABI Prism 7900  
634 sequence detection system (Thermo Scientific), using a SYBR® Green PCR Master Mix (Thermo  
635 Scientific).

636 *Ubiquitin10* (At4g05320) and *β-Tubulin* (Potri.011G162500) were used as housekeeping genes  
637 for *Arabidopsis* and poplar samples, respectively. All poplar primers were designed on *P.*

*trichocarpa* genome and the primer sequences for the genes analyzed is listed in Supporting Table S2.

Relative quantification of the expression of each gene was performed using the comparative threshold cycle method as described in Livak and Schmittgen (2001). Two technical replicates were used for each of the five biological samples and the data are representative of at least two independent experiments giving comparable profiles.

### **Confocal imaging**

Roots of seven-day-old seedlings were observed with the 20× objective of an Olympus FluoView1000 inverted confocal microscope. Green Fluorescent Protein (GFP) fluorescence was excited with 488-nm laser light (laser transmissivity -6%, photomultiplier voltage 650 V) and collected between 495 and 540 nm long-pass emission filter. Propidium iodide stain marking plant cell-walls was excited at 488 nm (laser transmissivity - 6%, PMT voltage 550V) and collected at 590–680 nm. Scanner and detector settings were kept unchanged during the whole experiment. Images were analysed with the Olympus FluoView FV1000 software.

### **Statistical analysis**

Statistical analysis was performed using GraphPad Prism version 6.00. According to the data sets, *t*-test, one-way or two-way ANOVA was conducted and differences between means were considered significant when the *p*-value was less than 0.05. In one-way ANOVA, the multiple comparisons of means were performed with the Tukey method, while in two-way ANOVA, via the Holm-Sidak method.

### **Supplemental Material**

**Supplemental Figure S1.** Core hypoxia-responsive genes are responsive to low oxygen in poplar.

**Supplemental Figure S2.** Occurrence of common motifs (CMV) in poplar and Arabidopsis ERF-VII proteins.

666 **Supplemental Figure S3.** Identification of the HRPE element in the promoter of poplar hypoxia-  
667 responsive genes.

668 **Supplemental Figure S4.** Transcriptional regulation of *Pop\_ERFB2-1* under Zn stress.

669 **Supplemental Table S1.** List of forward (5'→ 3') and reverse (5'→ 3') primer sequences for  
670 poplar coding sequences cloning.

671 **Supplemental Table S2.** List of forward (5'→ 3') and reverse (5'→ 3') primer sequences for  
672 poplar and Arabidopsis qPCR analysis.

673 **Supplemental Table S3.** List of differentially expressed genes in poplar or Arabidopsis under Zn  
674 excess and low oxygen conditions.

675 **Supplemental Table S4.** List of hypoxia-affected genes identified under Zn excess.

676 **Supplemental Table S5.** List of core hypoxia responsive genes affected by Zn excess.

677 **Supplemental Table S6.** Transcriptional regulation of poplar ERF-VIIIs under anoxia.

678 **Supplemental Table S7.** Transcriptional regulation of Arabidopsis hypoxia-responsive genes  
679 after 6 days of germination of Col-0 seeds, under iron starvation conditions.

680 **Supplemental Table S8.** Transcriptional regulation of Arabidopsis hypoxia-responsive genes  
681 under control and 1 mM Zn conditions for 2 days, in Col-0 and erf-VII mutant plants.

682 **Supplemental Table S9.** Fresh weight of *P. alba* 'Villafranca' plants under control, 1 mM Zn,  
683 waterlogging and a combination of 1 mM Zn and waterlogging conditions, for 4 days.

684 **Supplemental Table S10.** Dry weight of *P. alba* 'Villafranca' plants under control, 1 mM Zn,  
685 waterlogging and a combination of 1 mM Zn and waterlogging conditions, for 4 days.

686 **Supplemental Table S11.** Fresh weight of *P. alba* 'Villafranca' plants under control, 1 mM Zn,  
687 waterlogging and a combination of 1 mM Zn and waterlogging conditions, for 10 days.

688 **Supplemental Table S12.** Dry weight of *P. alba* 'Villafranca' plants under control, 1 mM Zn,

689 waterlogging and a combination of 1 mM Zn and waterlogging conditions, for 10 days.

690 **Supplemental Table S13.** Relative expression levels of metal transporters in poplar roots under  
691 Zn stress and waterlogging conditions.

692 **Supplemental Note S1.** Nucleotide and protein alignments of ERFB2-1 in *P. trichocarpa* and *P.*  
693 *alba* 'Villafranca'.

694 **Supplemental Note S2.** Alignment of Arabidopsis and poplar ERF-VII proteins.

695 **Supplemental Note S3.** Alignment of Arabidopsis and poplar PCO proteins.

696

## 697 **Acknowledgments**

698 We are grateful to Ms. Cristina Ghelardi, Ms. Francesca Vannucchi for assistance with poplar  
699 cultivation and to Ms. Gaia Monteforti for sharing her expertise in atomic absorption  
700 spectrophotometry. The authors declare no competing financial interests.

701



# Figure legends

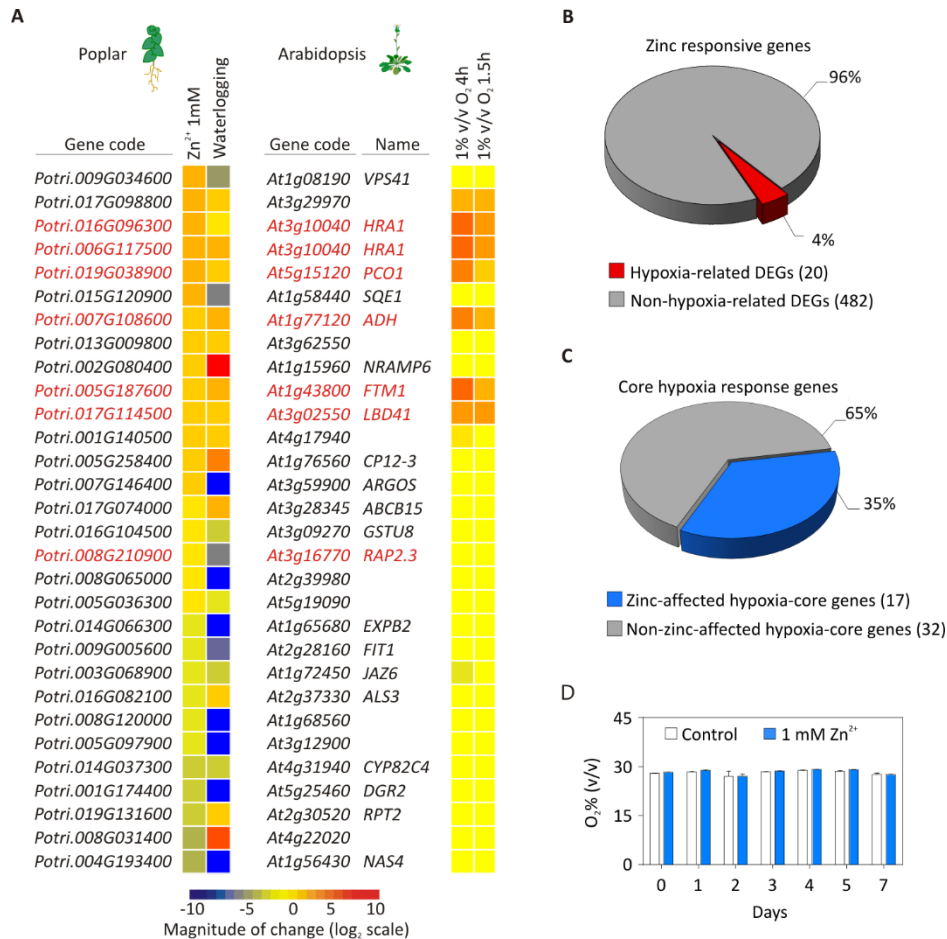


**Figure 1.** Molecular response to Zn overlaps with low-oxygen transcription regulation in poplar. A, Heat map showing common differentially expressed genes (DEGs) in poplar roots under 1 mM Zn(NO<sub>3</sub>)<sub>2</sub> (Ariani *et al.*, 2015), dataset defined by  $\chi^2$  test, Bonferroni corrected  $p$ -value < 0.1) and those genes altered after 168 h of soil hypoxia (Kreuzwieser *et al.*, 2009), compared to their Arabidopsis orthologs after 1.5 or 4 h hypoxia (1% v/v O<sub>2</sub>/N<sub>2</sub>) (Licausi *et al.*, 2010, 2011). In red are highlighted hypoxia-core genes. B, Percentage of hypoxia-affected genes identified among the total Zn DEGs (Ariani *et al.*, 2015), dataset defined by  $\chi^2$  test, not corrected  $p$ -value). C, Percentage of Zn-regulated genes in poplar that are also part of the core hypoxia-response genes. (d) Oxygen concentration (% v/v) measured in the hydroponic solution under control and 1 mM ZnSO<sub>4</sub> conditions for 7 days. Data are presented as mean  $\pm$  SD (n = 150).

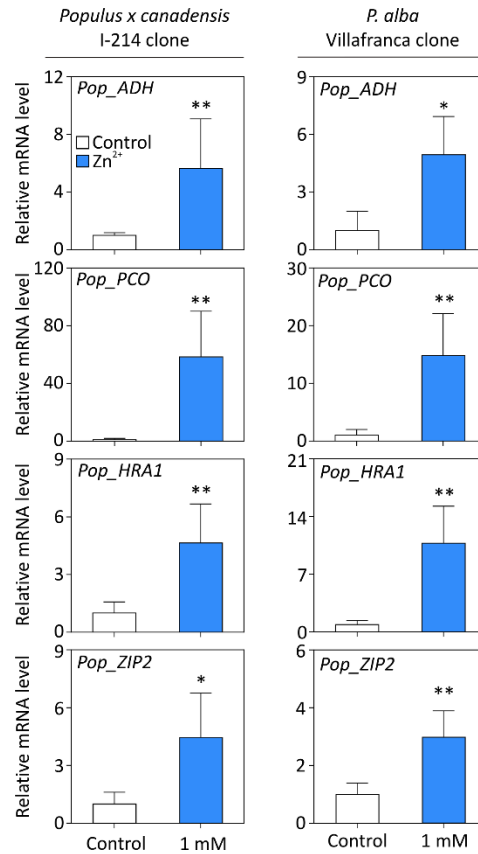


**Figure 2.** Zn excess promotes the molecular response to low-oxygen in poplar. Induction of hypoxia (*Pop\_ADH*, *Pop\_PCO* and *Pop\_HRA1*) and Zn (*Pop\_ZIP2*) marker genes in a Zn-sensitive (*Populus x canadensis* 'I-214' clone) and a Zn-tolerant (*P. alba* 'Villafranca' clone) poplar species, after 1 mM ZnSO<sub>4</sub> treatment for 21 days. Data are presented as mean ± SD (n = 5), two-tailed *t*-test, \* *p*-value < 0.05 and \*\* *p*-value < 0.01.

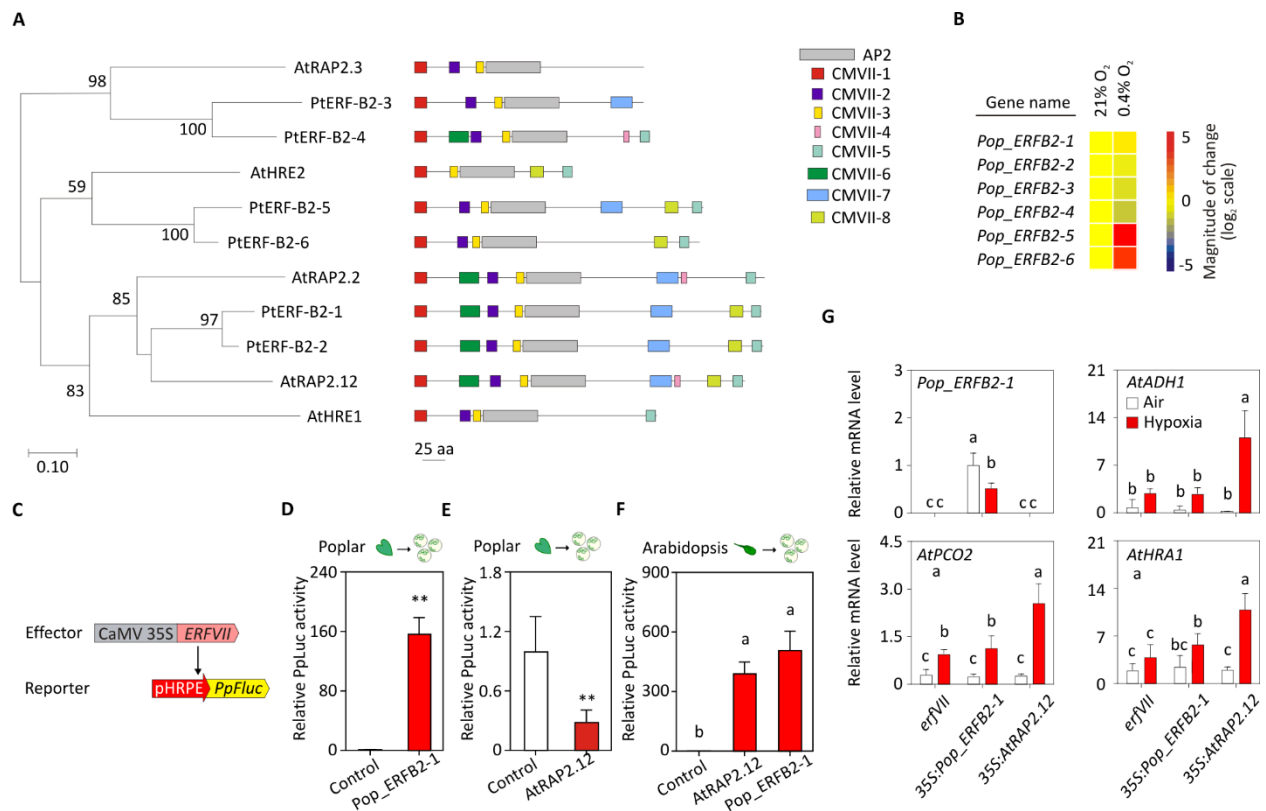


**Figure 3.** Characterization of the poplar ERF-VII protein, Pop\_ERFB2-1. A, Phylogenetic relationship between Arabidopsis ERF-VII and their best poplar orthologs (Zhuang *et al.*, 2008), generated from a multi-alignment processed via the maximum-likelihood algorithm. The ERF-VII common motifs (CMVIIs) are shown on the right of each sequence. B, Heat map showing relative expression of *Pop\_ERFB2*s under normoxic (21% v/v O<sub>2</sub>) and anoxic (0% v/v O<sub>2</sub>, 4h) conditions, in poplar roots. C, Graphic representation of the experiment conducted to collect the data shown in D, E and F. D, Effect of  $\Delta$ 13RAP2.12 on the synthetic hypoxia responsive promoter fused to the *Photinus pyralis* luciferase (*pHRPE:PpLuc*) in poplar protoplasts. Data are presented as mean + SD (n = 4), \*\* indicates *p*-value < 0.01, as calculated by two tailed *t*-test. E, Effect of GFP-Pop\_ERFB2-1 on *pHRPE:PpLuc* luciferase in poplar protoplasts. Data are presented as mean + SD (n = 4), \*\* indicates *p*-value < 0.01, as calculated by two tailed *t*-test. F, Effect of  $\Delta$ 13RAP2.12 and GFP-Pop\_ERFB2-1 on *pHRPE:PpLuc* luciferase in Arabidopsis protoplasts. Data are presented as mean + SD (n = 4), \*\* indicates *p*-value < 0.01, as calculated by two tailed *t*-test. G, Complementation of the Arabidopsis pentuple *erf-VII* mutant by the constitutive expression of *Pop\_ERFB2-1* and *AtRAP2.12*. Expression levels of *Pop\_ERFB2-1*,

738 *AtADH1*, *AtPCO2* and *AtHRA1* under aerobic (empty bars) and 6 h 1% v/v O<sub>2</sub> (red bars)  
739 conditions in the *erf-VII* background, *Pop\_ERB2-1* or *AtRAP2.12* expressing plants. Data are  
740 presented as mean + SD (n = 4), where values for *erf-VII* complemented lines correspond to the  
741 means of four independent lines. Letters mark statistically different averages as assessed by  
742 two-way ANOVA followed by Holm-Sidak post hoc test (*p*-value < 0.05).

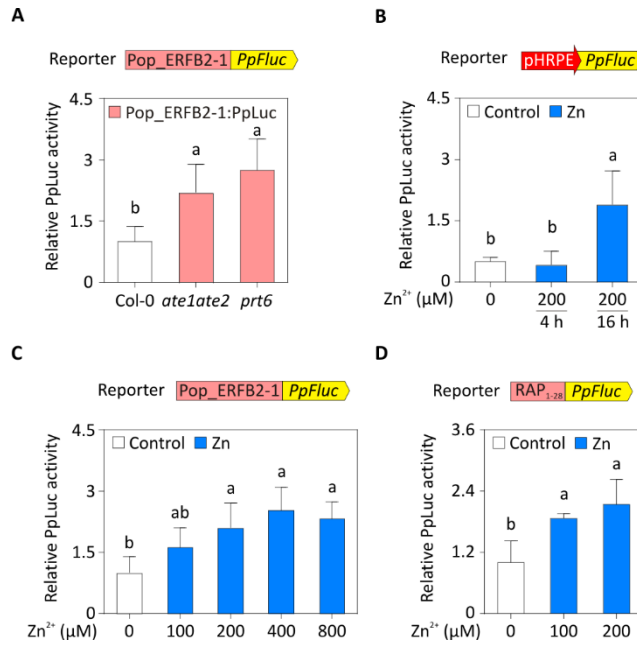


**Figure 4.** Zn effect on Pop\_ERFB2-1 stability and activity. A, Relative luciferase activity of PpLuc fused to Pop\_ERFB2-1, in protoplasts of wild type (Col-0) and *ate1ate2* and *prt6* Arabidopsis mutants. B, Effect of 200  $\mu$ M Zn on PpLuc expression driven by the *pHRPE* promoter after 4 or 16 h treatment in poplar protoplasts. C, Effect of an over-night treatment with a range of Zn concentrations (from 0 to 800  $\mu$ M) on Pop\_ERFB2-1-PpLuc activity in poplar protoplasts. D, Relative luciferase activity of PpLuc fused to the first 28 amino acids of Arabidopsis RAP2.12, after an overnight treatment with 100 or 200  $\mu$ M Zn, in Arabidopsis protoplasts. Data are shown as mean + SD (n = 5). Different letters indicate significant differences ( $p$ -value < 0.05, one-way ANOVA followed by Holm-Sidak post hoc test).

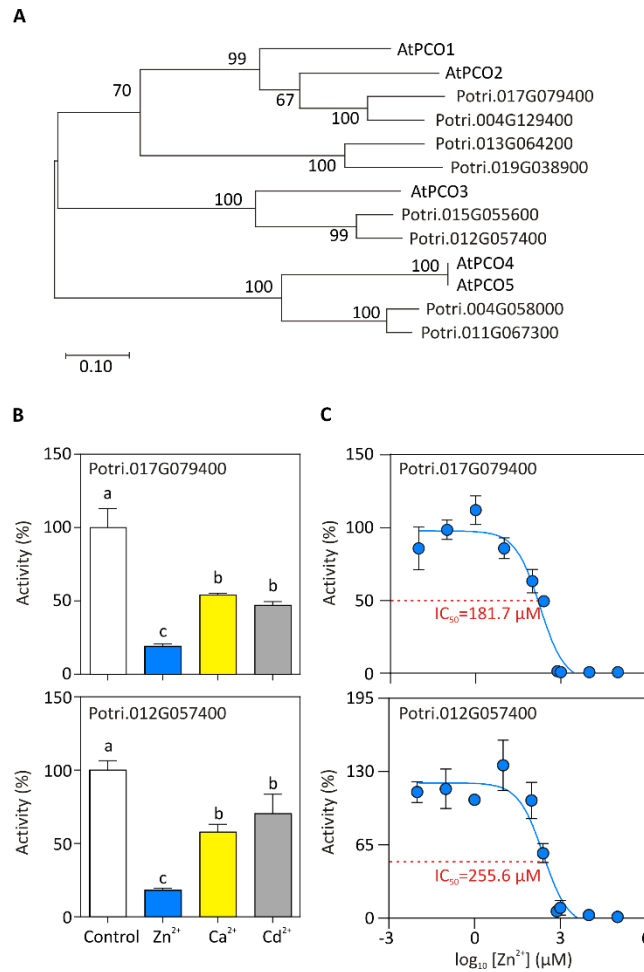
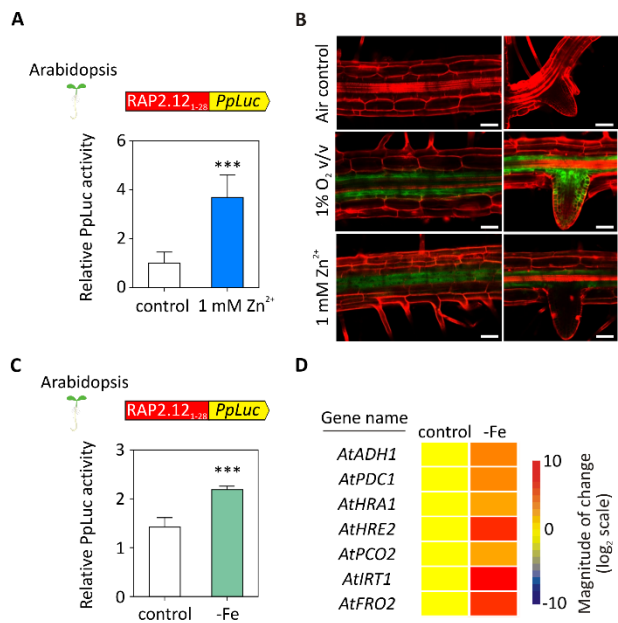


**Figure 5.** Zn<sup>2+</sup> exerts an inhibitory effect on poplar PCOs, *in vitro*. A, Phylogenetic tree of Plant Cysteine Oxidase (PCO) proteins from *A. thaliana* and *P. trichocarpa* generated from a multi-alignment processed via the maximum-likelihood algorithm. B, Activity inhibition of poplar PCOs Potri.012G057400 and Potri.017G079400 by different cations (Zn<sup>2+</sup>, Ca<sup>2+</sup> and Cd<sup>2+</sup>), using poplar Pop\_ERFB2-1 14 aa N-terminal peptide as substrate. Reactions were performed using 0.1 μM PCOs, 1 mM ERF, 100 μM metals, for 2 minutes. Data are presented as mean + se (n = 3). Results were analysed by one-way ANOVA followed by Tukey post-hoc test and different letters indicate significant differences (*p*-value < 0.05). C, Zn<sup>2+</sup> IC<sub>50</sub> fitting curves for poplar Potri.012G057400 and Potri.017G079400 activity on Pop\_ERFB2-1 14 aa N-terminal peptide. Zn<sup>2+</sup> effect on PCOs is expressed as enzyme activity (%) compared to control (100 %). Reactions were performed using 0.2 μM PCOs, for 2 minutes, metal concentrations are indicated in logarithmic scale. Data are presented as mean + s.e (n = 3).

766



767

768 **Figure 6.** Zn excess and iron starvation similarly induce hypoxia-like responses in Arabidopsis. A,  
769 Effect of 1 mM Zn on PpLuc activity in 8-day-old Arabidopsis seedlings stably expressing the  
770 MC-degron reporter *RAP2.12<sub>1-28</sub>-PpFluc* (Weits *et al.* 2014). Data are shown as mean + SD (n =  
771 5), \*\* indicate a *p*-value < 0.01, as assessed by two-tailed *t*-test. B, Laser-scanning confocal  
772 images of GFP fluorescent protein driven by the hypoxia-responsive synthetic promoter HPRE  
773 (*pHRPE:GFP*) in Arabidopsis roots under control (air control), hypoxia (1% O<sub>2</sub> v/v, 48 h) and Zn  
774 excess (1 mM ZnSO<sub>4</sub>, 48 h). Scale bar 100 μM. C, Effect of iron starvation on luciferase activity in  
775 6-day-old *RAP2.12<sub>1-28</sub>-PpFluc* transgenic seedlings. Data are shown as mean + SD (n = 5), \*\*\*  
776 indicate a *p*-value < 0.001, as assessed by two-tailed *t*-test. D, Heat map showing relative  
777 expression of hypoxia and Zn excess marker genes under control and iron starvation conditions,  
778 in 6-day-old Arabidopsis Col-0 seedlings.

779

780

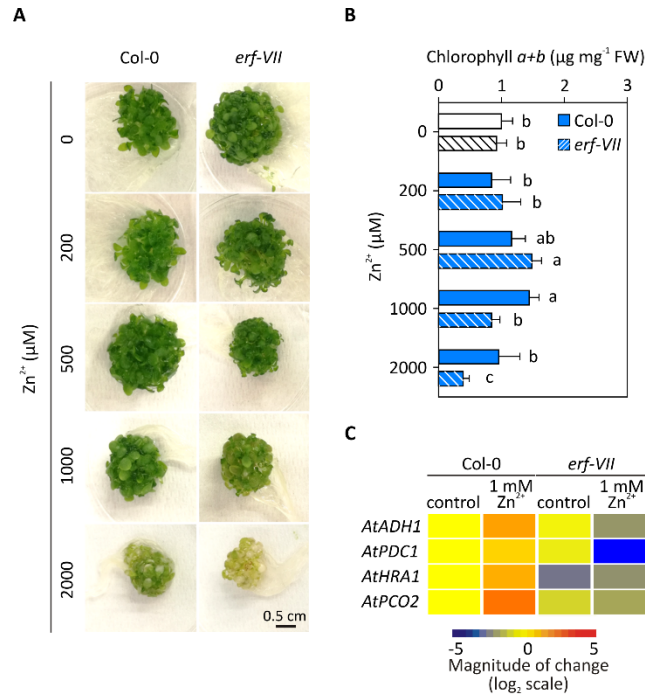
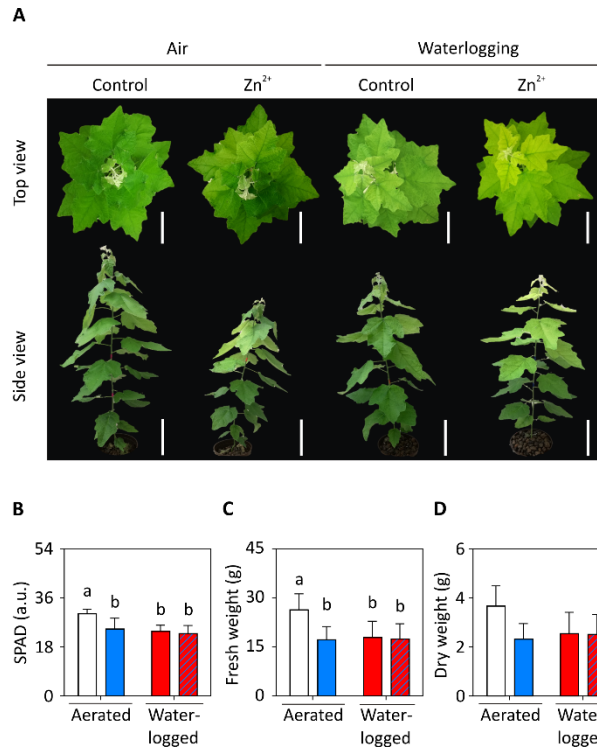


**Figure 7.** ERF-VIIs contribute to Arabidopsis tolerance to Zinc excess. A, 5-day-old wild type and *erf-VII* Arabidopsis seedlings were subjected to a range of Zn concentrations (from 0 to 2000 µM) for three days. Photos were taken at the end of the treatments and show a representative sample for each treatment. Scale bar 0.5 cm. B, Total chlorophyll quantification in wild type and *erf-VII* seedlings at the end of the treatment described in A. Data are presented as mean + SD (n = 6). Letters indicate statistically significant difference (*p*-value < 0.05, as assessed by two-way ANOVA followed by Holm-Sidak post-hoc test). C, Heat map displaying differential expression of hypoxia marker genes in response to 1 mM Zn in wild type and *erf-VII* seedlings, at the end of the treatments as described in A.





791

792 **Figure 8.** Effect of waterlogging and Zn stress on poplar phenotype. A, ‘Villafranca’ poplars were  
 793 subjected to 1 mM ZnSO<sub>4</sub> stress, to waterlogging and to a combination of the two, for 10 days.  
 794 Photos were taken at the end of the treatments and show a top view and a side view of a  
 795 representative plant for each treatment. Scale bar 15 cm. B, Total chlorophyll (SPAD units) in  
 796 leaves at the end of 10 days of the treatments described in A. Data are presented as mean + SD  
 797 (n = 10). Letters indicate statistically significant differences as assessed by two-way ANOVA  
 798 followed by Holm-Sidak post hoc test. (*p*-value < 0.05). C, Fresh weight of the total biomass of  
 799 plants after 10 days of the treatments described in A. D, Dry weight of the total biomass of  
 800 plants after 10 days of the treatments described in A. Data are presented as mean + SD (n = 5).  
 801 Letters indicate statistically significant differences as assessed by two-way ANOVA followed by  
 802 Holm-Sidak post hoc test (*p*-value < 0.05). White bar, control; blue bar, Zn treatment (1 mM  
 803 ZnSO<sub>4</sub>); red bar, root waterlogging treatment; red bar with blue stripes, combination of 1 mM  
 804 ZnSO<sub>4</sub> and waterlogging treatment.

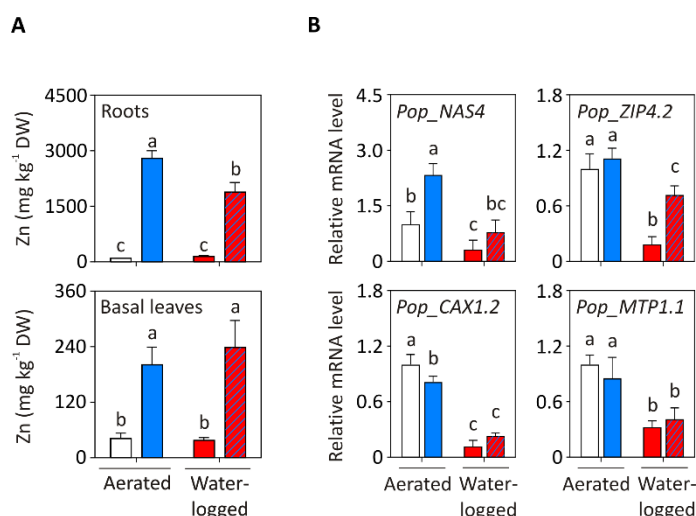


**Figure 9.** Zn uptake decreases in roots under waterlogging. A, Zn concentration (mg kg<sup>-1</sup> DW) in poplar roots and basal leaves after 10 days of the treatments described in Fig. 8. B, Relative expression levels of Zn transporters in poplar roots after 10 days of the treatments: *Pop\_NAS4* (*Potri.004G193400*), *Pop\_ZIP4.2* (*Potri.001G160400*), *Pop\_CAX1.2* (*Potri.009G045800*) and *Pop\_MTP1.1* (*Potri.014G106200*). All data are presented as mean + SD (n = 5). Letters indicate statistically significant differences as assessed by two-way ANOVA followed by Holm-Sidak post hoc test (*p*-value < 0.05). White bar, control; blue bar, Zn treatment (1 mM ZnSO<sub>4</sub>); red bar, root waterlogging treatment; red bar with blue stripes, combination of 1 mM ZnSO<sub>4</sub> and waterlogging treatment.

## Supplemental data legends

**Supplemental Figure S1.** Validation of low oxygen responsiveness of Arabidopsis homologs in poplar. Three putative hypoxia-responsive genes, *Pop\_PCO* (*Potri.019G038900*), *Pop\_ADH* (*Potri.007G108400*) and *Pop\_HRA1* (*Potri.006G117500*), were confirmed to respond to low oxygen (0.4% O<sub>2</sub> (v/v), 4 h) conditions in root tissue. Relative expression levels data are presented as mean ± SD (n = 5), *t*-test, \*\* *p*-value < 0.01.

**Supplemental Figure S2.** Occurrence of common motifs (CMV) in poplar and Arabidopsis ERF-VII proteins. (a) List of the consensus sequences of the CMV motifs present in the ERF-VII proteins, identified by Nakano et al. (2006). (b) Systematic comparison of the ERF-VII proteins from

826 Arabidopsis (Licausi et al. 2010) and *P. trichocarpa* (Zhuang et al. 2008), in terms of occurrence  
827 and position of the CMVII motifs.

828

829 **Supplemental Figure S3.** Identification of the HRPE element in the promoter of poplar hypoxia-  
830 responsive genes. Hypoxia Responsive Promoter Element (HRPE) was identified in the genomic  
831 region 2000 bp upstream of the translational starting site (ATG) of three poplar anaerobic  
832 genes: *Pop\_ADH* (*Potri.007G108400*), *Pop\_HRA1* (*Potri.006G117500*) and *Pop\_PCO*  
833 (*Potri.019G038900*), through FIMO algorithm. HRPE elements are highlighted in bold text and  
834 underlined with a single line, while the ATG is underlined with a double line.

835

836 **Supplemental Figure S4.** Transcriptional regulation of *Pop\_ERFB2-1* under Zn excess. Relative  
837 expression levels of poplar *Pop\_ERFB2-1* transcription factors under 1 mM Zn treatment  
838 compared to control conditions, in *P. alba* 'Villafranca' roots. Data are presented as mean (n =  
839 10) and SD, *t*-test (*p*-value < 0.05).

840

841 **Supplemental Table S1.** List of forward (5'→ 3') and reverse (5'→ 3') primer sequences for  
842 poplar coding sequences cloning.

843

844 **Supplemental Table S2.** List of forward (5'→ 3') and reverse (5'→ 3') primer sequences for  
845 poplar and Arabidopsis qPCR analysis.

846

847 **Supplemental Table S3.** List of differentially expressed genes in poplar and Arabidopsis under  
848 Zn excess or low oxygen conditions. Differentially expressed genes in poplar roots under 1 mM  
849 Zn(NO<sub>3</sub>)<sub>2</sub> (Ariani et al., 2015), dataset defined by  $\chi^2$  test, Bonferroni corrected *p*-value < 0.1) and  
850 those genes altered after 168 h of submergence (Kreuzwieser et al., 2009), compared to their

Arabidopsis orthologs after 1.5 or 4 h hypoxia (1% v/v O<sub>2</sub>/N<sub>2</sub>) (Licausi *et al.*, 2010, 2011). Data are presented as log<sub>2</sub>FC, followed by the *p*-value, for each dataset.

**Supplemental Table S4.** List of hypoxia-affected genes identified under Zn excess. The low oxygen responsive genes were identified among the total differentially regulated genes under 1 mM Zn treatment (Ariani *et al.*, 2015), dataset defined by  $\chi^2$  test, not corrected *p*-value).

**Supplemental Table S5.** List of core hypoxia responsive genes affected by Zn excess. Zn excess regulated genes (Ariani *et al.*, 2015), dataset defined by  $\chi^2$  test, not corrected *p*-value), which are also part of the core hypoxia response (Mustroph *et al.*, 2009) were identified in poplar comparing their best Arabidopsis orthologs.

**Supplemental Table S6.** Transcriptional regulation of poplar *ERF-VII*s under anoxia. Relative expression levels of poplar *ERF-VII* transcription factors under anoxic (0.4% O<sub>2</sub> (v/v)) compared to normoxic (21% O<sub>2</sub> (v/v)) conditions. Data are presented as mean (n = 5) and SD, *t*-test, significant *p*-value < 0.05 is shown in bold text.

**Supplemental Table S7.** Transcriptional regulation of Arabidopsis hypoxia-responsive genes after 6 days of germination of Col-0 seeds, under iron starvation conditions. Relative expression levels of Arabidopsis hypoxia-responsive genes under germination in iron-starved (0  $\mu$ M FeNaEDTA) compared to control (50  $\mu$ M FeNaEDTA) conditions. Data are presented as mean (n = 4) and SD, *t*-test, significant *p*-value < 0.05 is shown in bold text.

**Supplemental Table S8.** Transcriptional regulation of Arabidopsis hypoxia-responsive genes under control and 1 mM Zn conditions for 2 days, in Col-0 and *erf-VII* mutant plants. Relative expression levels of Arabidopsis hypoxia-responsive genes under Zn excess (1 mM ZnSO<sub>4</sub>) and control conditions. Data are presented as mean  $\pm$  SD (n = 4) and analyzed two-way ANOVA,

followed by Holm-Sidak post hoc test. Different letters indicate significant differences ( $p$ -value < 0.05).

**Supplemental Table S9.** Fresh weight of *P. alba* 'Villafranca' plants under control, 1 mM Zn, waterlogging and a combination of 1 mM Zn and waterlogging conditions, for 4 days. Values are presented as mean  $\pm$  SD ( $n = 5$ ). Data were analyzed by one-way ANOVA, followed by Tukey post hoc test and different letters indicate significant differences ( $p$ -value < 0.05).

**Supplemental Table S10.** Dry weight of *P. alba* 'Villafranca' plants under control, 1 mM Zn, waterlogging and a combination of 1 mM Zn and waterlogging conditions, for 4 days. Values are presented as mean  $\pm$  SD ( $n = 5$ ). Data were analyzed by one-way ANOVA, followed by Tukey post hoc test and different letters indicate significant differences ( $p$ -value < 0.05).

**Supplemental Table S11.** Fresh weight of *P. alba* 'Villafranca' plants under control, 1 mM Zn, waterlogging and a combination of 1 mM Zn and waterlogging conditions, for 10 days. Values are presented as mean  $\pm$  SD ( $n = 5$ ). Data were analyzed by two-way ANOVA, followed by Holm-Sidak post hoc test, and different letters indicate significant differences ( $p$ -value < 0.05).

**Supplemental Table S12.** Dry weight of *P. alba* 'Villafranca' plants under control, 1 mM Zn, waterlogging and a combination of 1 mM Zn and waterlogging conditions, for 10 days. Values are presented as mean  $\pm$  SD ( $n = 5$ ). Data were analyzed by two-way ANOVA, followed by Holm-Sidak post hoc test, and different letters indicate significant differences ( $p$ -value < 0.05).

**Supplemental Table S13.** Relative expression levels of metal transporters in poplar roots under Zn excess and waterlogging conditions. 'Villafranca' poplars were subjected to 1 mM ZnSO<sub>4</sub> stress, to waterlogging and to a combination of the two, for 10 days. Relative expression levels of Zn transporters were assessed in poplar roots at the end of the treatment. Data are presented as mean  $\pm$  SD ( $n = 5$ ), two-way ANOVA ( $p$ -value < 0.05 in bolt text).

906

907 **Supplemental Note S1.** Nucleotide and protein alignments of ERFB2-1 (Potri.003G071700) in *P.*  
908 *trichocarpa* and *P. alba* 'Villafranca'. The alignments (nucleotides (a) and amino acids (b)) were  
909 performed using ClustalO algorithm. ERFB2-1 from *P. trichocarpa* or *P. alba* 'Villafranca' are  
910 named PtERFB2-1 and Pop\_ERFB2-1, respectively.

911

912 **Supplemental Note S2.** Alignment showing the relationship between Arabidopsis ERF-VII and  
913 their best *P. trichocarpa* orthologs (Zhuang *et al.*, 2008), generated from a multi-alignment  
914 processed via the maximum-likelihood algorithm (MEGAX). Arabidopsis ERFs-VII: AtRAP2.2  
915 (At3g14230), AtRAP2.12 (At1t53910), AtRAP2.3 (At3g16770), AtHRE1 (At1g72360) and AtHRE2  
916 (At2g47520). Poplar ERFs-VII: PtERF-B2-1 (Potri.003G071700), PtERF-B2-2 (Potri.001G163700),  
917 PtERF-B2-3 (Potri.010G006800), PtERF-B2-4 (Potri.008G210900), PtERF-B2-5  
918 (Potri.002G201600), PtERF-B2-6 (Potri.014G126100).

919

920 **Supplemental Note S3.** Alignment of Arabidopsis and poplar Plant Cysteine Oxidase (PCO)  
921 proteins generated from a multi-alignment processed via the maximum-likelihood algorithm  
922 (MEGAX). Arabidopsis PCOs: AtPCO1 (At5g15120), AtPCO2 (At5g39890), AtPCO3 (At1g18490),  
923 AtPCO4 (At2g42670) and AtPCO5 (At2g42670). Poplar PCOs: Potri.017G079400,  
924 Potri.004G129400, Potri.013G064200, Potri.019G038900, Potri.004G058000,  
925 Potri.011G067300, Potri.015G055600 and Potri.012G057400.

926

927

## Parsed Citations

**Abbas M, Berckhan S, Rooney DJ, Gibbs DJ, Vicente Conde J, Sousa Correia C, Bassel GW, Marín-De La Rosa N, León J, Alabadí D, et al. 2015. Oxygen sensing coordinates photomorphogenesis to facilitate seedling survival. *Current Biology* 25: 1483–1488.**

Pubmed: [Author and Title](#)

Google Scholar: [Author Only](#) [Title Only](#) [Author and Title](#)

**Abdullah AS. 2015. Zinc availability and dynamics in the transition from flooded to aerobic rice cultivation. *Journal of Plant Biology & Soil Health* 2: 1–5.**

Pubmed: [Author and Title](#)

Google Scholar: [Author Only](#) [Title Only](#) [Author and Title](#)

**Altschul SF, Gish W, Miller W, Myers EW, Lipman DJ. 1990. Basic local alignment search tool. *Journal of molecular biology* 215: 403–10.**

Pubmed: [Author and Title](#)

Google Scholar: [Author Only](#) [Title Only](#) [Author and Title](#)

**Ariani A, Di Baccio D, Romeo S, Lombardi L, Andreucci A, Lux A, Horner DS, Sebastiani L. 2015. RNA sequencing of *Populus x canadensis* roots identifies key molecular mechanisms underlying physiological adaption to excess zinc. *Plos One* 10: e0117571.**

Pubmed: [Author and Title](#)

Google Scholar: [Author Only](#) [Title Only](#) [Author and Title](#)

**Di Baccio D, Kopriva S, Sebastiani L, Rennenberg H. 2005. Does glutathione metabolism have a role in the defence of poplar against zinc excess? *New Phytologist* 167: 73–80.**

Pubmed: [Author and Title](#)

Google Scholar: [Author Only](#) [Title Only](#) [Author and Title](#)

**Di Baccio D, Tognetti R, Minnocci A, Sebastiani L. 2009. Responses of the *Populus x euramericana* clone I-214 to excess zinc: Carbon assimilation, structural modifications, metal distribution and cellular localization. *Environmental and Experimental Botany* 67: 153–163.**

Pubmed: [Author and Title](#)

Google Scholar: [Author Only](#) [Title Only](#) [Author and Title](#)

**Di Baccio D, Tognetti R, Sebastiani L, Vitagliano C. 2003. Responses of *Populus deltoides* x *Populus nigra* (*Populus x euramericana*) clone I-214 to high zinc concentrations. *New Phytologist* 159: 443–452.**

Pubmed: [Author and Title](#)

Google Scholar: [Author Only](#) [Title Only](#) [Author and Title](#)

**Banti V, Giuntoli B, Gonzali S, Loreti E, Magneschi L, Novi G, Paparelli E, Parlanti S, Pucciariello C, Santaniello A, et al. 2013. Low oxygen response mechanisms in green organisms. *International Journal of Molecular Sciences* 14: 4734–4761.**

Pubmed: [Author and Title](#)

Google Scholar: [Author Only](#) [Title Only](#) [Author and Title](#)

**Bouain N, Shahzad Z, Rouached A, Khan GA, Berthomieu P, Abdely C, Poirier Y, Rouached H. 2014. Phosphate and zinc transport and signalling in plants: Toward a better understanding of their homeostasis interaction. *Journal of Experimental Botany* 65: 5725–5741.**

Pubmed: [Author and Title](#)

Google Scholar: [Author Only](#) [Title Only](#) [Author and Title](#)

**Broadley MR, White PJ, Hammond JP, Zelko I, Lux A. 2007. Zinc in plants: Tansley review. *New Phytologist* 173: 677–702.**

Pubmed: [Author and Title](#)

Google Scholar: [Author Only](#) [Title Only](#) [Author and Title](#)

**Bui LT, Giuntoli B, Kosmacz M, Parlanti S, Licausi F. 2015. Constitutively expressed ERF-VII transcription factors redundantly activate the core anaerobic response in *Arabidopsis thaliana*. *Plant Science* 236: 37–43.**

Pubmed: [Author and Title](#)

Google Scholar: [Author Only](#) [Title Only](#) [Author and Title](#)

**Ciszewski D, Grygar TM. 2016. A review of flood-related storage and remobilization of heavy metal pollutants in river systems. *Water, Air, and Soil Pollution* 227.**

Pubmed: [Author and Title](#)

Google Scholar: [Author Only](#) [Title Only](#) [Author and Title](#)

**Clough SJ, Bent AF. 1998. Floral dip: A simplified method for *Agrobacterium*-mediated transformation of *Arabidopsis thaliana*. *Plant Journal* 16: 735–743.**

Pubmed: [Author and Title](#)

Google Scholar: [Author Only](#) [Title Only](#) [Author and Title](#)

**Coleman JE. 1998. Zinc enzymes. *Current Opinion in Chemical Biology* 2: 222–234.**

Pubmed: [Author and Title](#)

Google Scholar: [Author Only](#) [Title Only](#) [Author and Title](#)

**Dinneny JR, Long TA, Wang JY, Jung JW, Mace D, Pointer S, Barron C, Brady SM, Schiefelbein J, Benfey PN. 2008. Cell identity mediates the response of *Arabidopsis* roots to abiotic stress. *Science* 320: 942–5.**

Pubmed: [Author and Title](#)

Google Scholar: [Author Only](#) [Title Only](#) [Author and Title](#)

van Dongen JT, Licausi F. 2015. Oxygen Sensing and Signaling. *Annual Review of Plant Biology* 66: 345–367.

Pubmed: [Author and Title](#)

Google Scholar: [Author Only](#) [Title Only](#) [Author and Title](#)

Dudev T, Nikolova V. 2016. Determinants of Fe<sup>2+</sup> over M<sup>2+</sup> (M = Mg, Mn, Zn) selectivity in non-heme iron proteins. *Inorganic Chemistry* 55: 12644–12650.

Pubmed: [Author and Title](#)

Google Scholar: [Author Only](#) [Title Only](#) [Author and Title](#)

Edgar RC. 2004. MUSCLE: Multiple sequence alignment with high accuracy and high throughput. *Nucleic Acids Research* 32: 1792–1797.

Pubmed: [Author and Title](#)

Google Scholar: [Author Only](#) [Title Only](#) [Author and Title](#)

Gasch P, Funderinger M, Müller JT, Lee T, Bailey-Serres J, Mustroph A. 2015. Redundant ERF-VII transcription factors bind an evolutionarily-conserved cis-motif to regulate hypoxia-responsive gene expression in Arabidopsis. *The Plant Cell* 28: 160–180.

Pubmed: [Author and Title](#)

Google Scholar: [Author Only](#) [Title Only](#) [Author and Title](#)

Gibbs J, Greenway H. 2003. Mechanisms of anoxia tolerance in plants. I. Growth, survival and anaerobic catabolism. *Functional Plant Biology* 30: 1–47.

Pubmed: [Author and Title](#)

Google Scholar: [Author Only](#) [Title Only](#) [Author and Title](#)

Gibbs DJ, Lee SC, Isa N, Gramuglia S, Fukao T, Bassel GW, Correia CS, Corbineau F, Theodoulou FL, Bailey-serres J, et al. 2011. Homeostatic response to hypoxia is regulated by N-end rule pathway in plants. *Nature* 479: 415–418.

Pubmed: [Author and Title](#)

Google Scholar: [Author Only](#) [Title Only](#) [Author and Title](#)

Gibbs DJ, Mdlsa N, Movahedi M, Lozano-Juste J, Mendiondo GM, Berckhan S, Marin-de-laRosa N, VicenteConde J, SousaCorreia C, Pearce SP, et al. 2014. Nitric oxide sensing in plants is mediated by proteolytic control of group VII ERF transcription factors. *Molecular Cell* 53: 369–79.

Pubmed: [Author and Title](#)

Google Scholar: [Author Only](#) [Title Only](#) [Author and Title](#)

Giuntoli B, Shukla V, Maggiorelli F, Giorgi FM, Lombardi L, Perata P, Licausi F. 2017. Age-dependent regulation of ERF-VII transcription factor activity in Arabidopsis thaliana. *Plant, Cell & Environment* 40: 2333–2346.

Pubmed: [Author and Title](#)

Google Scholar: [Author Only](#) [Title Only](#) [Author and Title](#)

Graciet E, Wellmer F. 2010. The plant N-end rule pathway: Structure and functions. *Trends in Plant Science* 15: 447–453.

Pubmed: [Author and Title](#)

Google Scholar: [Author Only](#) [Title Only](#) [Author and Title](#)

Irving H, Williams RJP. 1948. Order of stability of metal complexes. *Nature* 162: 746–747.

Pubmed: [Author and Title](#)

Google Scholar: [Author Only](#) [Title Only](#) [Author and Title](#)

Isebrands JG, Richardson J. 2014. Poplars and willows: trees for society and the environment. CABI.

Pubmed: [Author and Title](#)

Google Scholar: [Author Only](#) [Title Only](#) [Author and Title](#)

Kosmacz M, Parlanti S, Schwarzländer M, Kragler F, Licausi F, Van Dongen JT. 2015. The stability and nuclear localization of the transcription factor RAP2.12 are dynamically regulated by oxygen concentration. *Plant, Cell and Environment* 38: 1094–1103.

Pubmed: [Author and Title](#)

Google Scholar: [Author Only](#) [Title Only](#) [Author and Title](#)

Kreuzwieser J, Furniss S, Rennenberg H. 2002. Impact of waterlogging on the N-metabolism of flood tolerant and non-tolerant tree species. *Plant, Cell and Environment* 25: 1039–1049.

Pubmed: [Author and Title](#)

Google Scholar: [Author Only](#) [Title Only](#) [Author and Title](#)

Kreuzwieser J, Hauberg J, Howell KA, Carroll A, Rennenberg H, Millar AH, Whelan J. 2009. Differential response of gray poplar leaves and roots underpins stress adaptation during hypoxia. *Plant Physiology* 149: 461–473.

Pubmed: [Author and Title](#)

Google Scholar: [Author Only](#) [Title Only](#) [Author and Title](#)

Kumar S, Stecher G, Li M, Knyaz C, Tamura K. 2018. MEGA X: molecular evolutionary genetics analysis across computing platforms. *Molecular biology and evolution* 35: 1547–1549.

Pubmed: [Author and Title](#)

Google Scholar: [Author Only](#) [Title Only](#) [Author and Title](#)

Lanquar V, Grossmann G, Vinkenberg JL, Merckx M, Thomine S, Frommer WB. 2014. Dynamic imaging of cytosolic zinc in Arabidopsis roots combining FRET sensors and RootChip technology. *New Phytologist* 202: 198–208.

Pubmed: [Author and Title](#)



Google Scholar: [Author Only](#) [Title Only](#) [Author and Title](#)

Lanquar V, Ramos MS, Lelièvre F, Ne Barbier-Brygoo H, Krieger-Liszak A, Krämer U, Thomine S. 2010. Export of vacuolar manganese by AtNRAMP3 and AtNRAMP4 is required for optimal photosynthesis and growth under manganese deficiency. *Plant physiology* 52: 1986–99.

Pubmed: [Author and Title](#)

Google Scholar: [Author Only](#) [Title Only](#) [Author and Title](#)

Licausi F, Van Dongen JT, Giuntoli B, Novi G, Santaniello A, Geigenberger P, Perata P. 2010. HRE1 and HRE2, two hypoxia-inducible ethylene response factors, affect anaerobic responses in *Arabidopsis thaliana*. *Plant Journal* 62: 302–315.

Pubmed: [Author and Title](#)

Google Scholar: [Author Only](#) [Title Only](#) [Author and Title](#)

Licausi F, Kosmacz M, Weits DA, Giuntoli B, Giorgi FM, Voesenek LACJ, Perata P, Van Dongen JT. 2011. Oxygen sensing in plants is mediated by an N-end rule pathway for protein destabilization. *Nature* 479: 419–422.

Pubmed: [Author and Title](#)

Google Scholar: [Author Only](#) [Title Only](#) [Author and Title](#)

Livak KJ, Schmittgen TD. 2001. Analysis of relative gene expression data using real-time quantitative PCR and the 2- $\Delta\Delta C_T$  method. *Methods* 25: 402–408.

Pubmed: [Author and Title](#)

Google Scholar: [Author Only](#) [Title Only](#) [Author and Title](#)

Lichtenthaler HK. 1987. Chlorophylls and carotenoids: pigments of photosynthetic membranes. *Methods in enzymology* 148: 350–382.

Pubmed: [Author and Title](#)

Google Scholar: [Author Only](#) [Title Only](#) [Author and Title](#)

Long XX, Yang XE, Ni WZ, Ye ZQ, He ZL, Calvert D V, Stoffella JP. 2003. Assessing zinc thresholds for phytotoxicity and potential dietary toxicity in selected vegetable crops. *Communications In Soil Science And Plant Analysis* 34: 10016.

Pubmed: [Author and Title](#)

Google Scholar: [Author Only](#) [Title Only](#) [Author and Title](#)

Loreti E, Valeri MC, Novi G, Perata P. 2018. Gene regulation and survival under hypoxia requires starch availability and metabolism. *Plant physiology* 176: 1286–1298.

Pubmed: [Author and Title](#)

Google Scholar: [Author Only](#) [Title Only](#) [Author and Title](#)

Lumba S, Toh S, Handfield L-F, Swan M, Liu R, Youn J-Y, Cutler SR, Subramaniam R, Provart N, Moses A, et al. 2014. A mesoscale abscisic acid hormone interactome reveals a dynamic signaling landscape in *Arabidopsis*. *Developmental Cell* 29: 360–372.

Pubmed: [Author and Title](#)

Google Scholar: [Author Only](#) [Title Only](#) [Author and Title](#)

Maret W. 2013. Inhibitory zinc sites in enzymes. *BioMetals* 26: 197–204.

Pubmed: [Author and Title](#)

Google Scholar: [Author Only](#) [Title Only](#) [Author and Title](#)

Müller A, Volmer K, Mishra-Knyrim M, Polle A. 2013. Growing poplars for research with and without mycorrhizas. *Frontiers in plant science* 4: 332.

Pubmed: [Author and Title](#)

Google Scholar: [Author Only](#) [Title Only](#) [Author and Title](#)

Murashige T, Skoog F. 1962. A revised medium for rapid growth and bio assays with tobacco tissue cultures. *Physiologia Plantarum* 15: 473–497.

Pubmed: [Author and Title](#)

Google Scholar: [Author Only](#) [Title Only](#) [Author and Title](#)

Mustroph A, Zanetti ME, Jang CJH, Holtan HE, Repetti PP, Galbraith DW, Girke T, Bailey-Serres J. 2009. Profiling transcriptomes of discrete cell populations resolves altered cellular priorities during hypoxia in *Arabidopsis*. *Proceedings of the National Academy of Sciences of the United States of America* 106: 18843–8.

Pubmed: [Author and Title](#)

Google Scholar: [Author Only](#) [Title Only](#) [Author and Title](#)

Olsen LI, Palmgren MG. 2014. Many rivers to cross: the journey of zinc from soil to seed. *Frontiers in Plant Science* 5: 30.

Pubmed: [Author and Title](#)

Google Scholar: [Author Only](#) [Title Only](#) [Author and Title](#)

Ou B, Yin K-Q, Liu S-N, Yang Y, Gu T, Wing Hui JM, Zhang L, Miao J, Kondou Y, Matsui M, et al. 2011. A high-throughput screening system for *Arabidopsis* transcription factors and its application to Med25-dependent transcriptional regulation. *Molecular Plant* 4: 546–555.

Pubmed: [Author and Title](#)

Google Scholar: [Author Only](#) [Title Only](#) [Author and Title](#)

Pajevi S, Bori M, Arsenov DD, Milan Ž. 2016. Phytoextraction of heavy metals by fast-growing trees: A review. In: *Phytoremediation*. Springer, 29–65.

Pubmed: [Author and Title](#)

**Pilon-Smits E. 2005. Phytoremediation. Annual Review of Plant Biology 56: 15–39.**

Pubmed: [Author and Title](#)

Google Scholar: [Author Only](#) [Title Only](#) [Author and Title](#)

**Ranjan A, Dickopf S, Ullrich KK, Rensing SA, Hoecker U. 2014. Functional analysis of COP1 and SPA orthologs from Physcomitrella and rice during photomorphogenesis of transgenic Arabidopsis reveals distinct evolutionary conservation. BMC Plant Biology 14: 178.**

Pubmed: [Author and Title](#)

Google Scholar: [Author Only](#) [Title Only](#) [Author and Title](#)

**Ricachenevsky FK, Menguer PK, Sperotto RA, Fett JP. 2015. Got to hide your Zn away: Molecular control of Zn accumulation and biotechnological applications. Plant Science 236: 1–17.**

Pubmed: [Author and Title](#)

Google Scholar: [Author Only](#) [Title Only](#) [Author and Title](#)

**Romeo S, Francini A, Ariani A, Sebastiani L. 2014. Phytoremediation of Zn: Identify the diverging resistance, uptake and biomass production behaviours of poplar clones under high zinc stress. Water, Air, and Soil Pollution 225: 1–12.**

Pubmed: [Author and Title](#)

Google Scholar: [Author Only](#) [Title Only](#) [Author and Title](#)

**Romeo S, Francini A, Sebastiani L, Morabito D. 2017. High Zn concentration does not impair biomass, cutting radial growth, and photosynthetic activity traits in Populus alba L. Journal of Soils and Sediments 17: 1394–1402.**

Pubmed: [Author and Title](#)

Google Scholar: [Author Only](#) [Title Only](#) [Author and Title](#)

**Sasidharan R, Hartman S, Liu Z, Martopawiro S, Sajeev N, van Veen H, Yeung E, Voesenek LACJ. 2018. Signal dynamics and interactions during flooding stress. Plant physiology 176: 1106–1117.**

Pubmed: [Author and Title](#)

Google Scholar: [Author Only](#) [Title Only](#) [Author and Title](#)

**Schuler M, Bauer P. 2011. Heavy metals need assistance: The contribution of nicotianamine to metal circulation throughout the plant and the Arabidopsis NAS gene family. Frontiers in Plant Science 2: 1–5.**

Pubmed: [Author and Title](#)

Google Scholar: [Author Only](#) [Title Only](#) [Author and Title](#)

**Sebastiani L, Francini A, Romeo S, Ariani A, Minnocci A. 2014. Heavy Metals Stress on Poplar: Molecular and Anatomical Modifications. In: Approaches to Plant Stress and their Management. New Delhi: Springer India, 267–279.**

Pubmed: [Author and Title](#)

Google Scholar: [Author Only](#) [Title Only](#) [Author and Title](#)

**Sharma SS, Dietz KJ, Mimura T. 2016. Vacuolar compartmentalization as indispensable component of heavy metal detoxification in plants. Plant Cell and Environment 39: 1112–1126.**

Pubmed: [Author and Title](#)

Google Scholar: [Author Only](#) [Title Only](#) [Author and Title](#)

**Shahzad Z, Canut M, Tournaire-Roux C, Martinière A, Boursiac Y, Loudet O, Maurel C. 2016. A potassium-dependent oxygen sensing pathway regulates plant root hydraulics. Cell 167: 87–98.**

Pubmed: [Author and Title](#)

Google Scholar: [Author Only](#) [Title Only](#) [Author and Title](#)

**Shi WG, Li H, Liu TX, Polle A, Peng CH, Luo Z Bin. 2015. Exogenous abscisic acid alleviates zinc uptake and accumulation in Populus × canescens exposed to excess zinc. Plant Cell and Environment 38: 207–223.**

Pubmed: [Author and Title](#)

Google Scholar: [Author Only](#) [Title Only](#) [Author and Title](#)

**Sinclair SA, Krämer U. 2012. The zinc homeostasis network of land plants. Biochimica et Biophysica Acta - Molecular Cell Research 1823: 1553–1567.**

Pubmed: [Author and Title](#)

Google Scholar: [Author Only](#) [Title Only](#) [Author and Title](#)

**Sivitz AB, Hermand V, Curie C, Vert G. 2012. Arabidopsis bHLH100 and bHLH101 control iron homeostasis via a FIT-independent pathway (M Bennett, Ed.). PLoS ONE 7: e44843.**

Pubmed: [Author and Title](#)

Google Scholar: [Author Only](#) [Title Only](#) [Author and Title](#)

**Tripathy BC, Pattanayak GK. 2012. Chlorophyll Biosynthesis in Higher Plants. In: Photosynthesis. Advances in Photosynthesis and Respiration. Springer, Dordrecht, 63–94.**

Pubmed: [Author and Title](#)

Google Scholar: [Author Only](#) [Title Only](#) [Author and Title](#)

**Tsednee M, Yang S, Lee D, Yeh K. 2014. Root-secreted nicotianamine from Arabidopsis halleri facilitates zinc hypertolerance by regulating zinc bioavailability. Plant physiology 166: 839–852.**

Pubmed: [Author and Title](#)

Google Scholar: [Author Only](#) [Title Only](#) [Author and Title](#)

**Vicente J, Mendiando GM, Movahedi M, Peirats-Llobet M, Juan Y ting, Shen Y yen, Dambire C, Smart K, Rodriguez PL, Charng Y yung, et al. 2017. The Cys-Arg/N-end rule pathway is a general sensor of abiotic stress in flowering plants. Current Biology 27: 3183–3190.e4.**

Pubmed: [Author and Title](#)

Google Scholar: [Author Only](#) [Title Only](#) [Author and Title](#)

**Varshavsky A. 2019. N-degron and C-degron pathways of protein degradation. Proceedings of the National Academy of Sciences 116: 358–366.**

Pubmed: [Author and Title](#)

Google Scholar: [Author Only](#) [Title Only](#) [Author and Title](#)

**Weits DA, Giuntoli B, Kosmacz M, Parlanti S, Hubberten HM, Riegler H, Hoefgen R, Perata P, Van Dongen JT, Licausi F. 2014. Plant cysteine oxidases control the oxygen-dependent branch of the N-end-rule pathway. Nature Communications 8: 14690.**

Pubmed: [Author and Title](#)

Google Scholar: [Author Only](#) [Title Only](#) [Author and Title](#)

**Weits DA, Kunkowska, Alicja B. Kamps NCW, Portz K, Packbier, Niko K. Nemec-Venza Z, Gaillochot, Christophe Lohmann JU, Pedersen O, van Dongen, Joost T. Licausi F. An apical hypoxic niche sets the pace over shoot meristem activity. Nature.**

**White MD, Flashman E. 2016. Catalytic strategies of the non-heme iron dependent oxygenases and their roles in plant biology. Current Opinion in Chemical Biology 31: 126–135.**

Pubmed: [Author and Title](#)

Google Scholar: [Author Only](#) [Title Only](#) [Author and Title](#)

**White MD, Kamps JJAG, East S, Taylor Kearney LJ, Flashman E. 2018. The plant cysteine oxidases from Arabidopsis thaliana are kinetically tailored to act as oxygen sensors. The Journal of biological chemistry 293: 11786–11795.**

Pubmed: [Author and Title](#)

Google Scholar: [Author Only](#) [Title Only](#) [Author and Title](#)

**White MD, Klecker M, Hopkinson RJ, Weits DA, Mueller C, Naumann C, O'Neill R, Wickens J, Yang J, Brooks-Bartlett JC, et al. 2017. Plant cysteine oxidases are dioxygenases that directly enable arginyl transferase-catalysed arginylation of N-end rule targets. Nature Communications 8: 14690.**

Pubmed: [Author and Title](#)

Google Scholar: [Author Only](#) [Title Only](#) [Author and Title](#)

**Wu K, Tian L, Hollingworth J, Brown DCW, Miki B. 2002. Functional analysis of tomato Pti4 in Arabidopsis. Plant physiology 128: 30–7.**

Pubmed: [Author and Title](#)

Google Scholar: [Author Only](#) [Title Only](#) [Author and Title](#)

**Yadav SK. 2010. Heavy metals toxicity in plants: An overview on the role of glutathione and phytochelatin in heavy metal stress tolerance of plants. South African Journal of Botany 76: 167–179.**

Pubmed: [Author and Title](#)

Google Scholar: [Author Only](#) [Title Only](#) [Author and Title](#)

**Yoo S-D, Cho Y-H, Sheen J. 2007. Arabidopsis mesophyll protoplasts: a versatile cell system for transient gene expression analysis. Nature Protocols 2: 1565–1572.**

Pubmed: [Author and Title](#)

Google Scholar: [Author Only](#) [Title Only](#) [Author and Title](#)

**Zhuang J, Cai B, Peng RH, Zhu B, Jin XF, Xue Y, Gao F, Fu XY, Tian YS, Zhao W, et al. 2008. Genome-wide analysis of the AP2/ERF gene family in Populus trichocarpa. Biochemical and Biophysical Research Communications 371: 468–474**

Pubmed: [Author and Title](#)

Google Scholar: [Author Only](#) [Title Only](#) [Author and Title](#)